Spring 5-15-2023

3-Dimensional Visualization of Cardiac Plaque Mapping Data

Phan Ly Vy Nguyen

WASHINGTON UNIVERSITY IN ST. LOUIS

McKelvey School of Engineering
Department of Biomedical Engineering

Thesis Examination Committee:
Christian Zemlin, Chair
Jonathan R. Silva
Chao Zhou

3-Dimensional Visualization of Cardiac Plaque Mapping Data

by

Phan Ly Vy Nguyen

A thesis presented to the McKelvey School of Engineering of Washington University in partial fulfillment of the requirements for the degree of Master of Science

May 2023
St. Louis, Missouri

Table of Contents

List of Figures

List of Tables

List of Abbreviations

2D – 2-dimensional

3D – 3-dimensional

AF – Atrial Fibrillation

AV – Atrioventricular

BCL – Basic Cycle Length

ECG – Electrocardiogram

ECGI – Electrocardiographic Imaging

GUI – Graphical User Interface

LP – Left Posterior

OR – Operation Room

RAA – Right Atrial Appendage

RP – Right Posterior

SA – Sinoatrial

Acknowledgments

I would like to express my sincere gratitude to Dr. Christian Zemlin for his guidance, encouragement, and support throughout the entire process of this study. His insights were crucial in shaping the direction of my research and in ensuring that the study remained focused.

I would also like to extend my appreciation to our lab research technician, Nick Razo, for his advice in designing the study and his assistance in the data analysis process. His assistance has been very helpful in guiding my research.

Finally, I would also like to thank Dr. Martha McGilvray, the resident in Cardiac Surgery, for her invaluable contribution to this study. Dr. McGilvray and Nick played a key role in collecting and providing the data for the study. Without their contribution, this study would not have been possible.

Phan Ly Vy Nguyen

Washington University in St. Louis

May 2023

Dedicated to my beloved parents, whose constant love, support, and encouragement have made it possible for me to succeed in my academic endeavors. I am grateful for their unwavering faith in me, which has been my greatest source of strength.

Dedicated to my friends at Knox College, whose companions and constant support has given me the strength to persist and overcome the challenges along the way.

.

ABSTRACT OF THE THESIS

3-Dimensional Visualization of Cardiac Plaque Mapping Data

by

Phan Ly Vy Nguyen

Master of Science in Biomedical Engineering

Washington University in St. Louis, 2023

Associate Professor Christian Zemlin, Chair

Atrial Fibrillation (AF) of one of the most prevalent cardiac arrythmia in humans, and also the most studied arrythmias due to its high association with cardiovascular morbidity and mortality. Diagnosis of AF, which is highly dependent on the observation of the irregular signal in the atria, is often challenging since AF is often asymptomatic at the onset. There has been a lot of effort in exploring different cardiac mapping techniques to understand the dynamics of AF for better intervention. This study aims at developing a MATLAB interface that assists the development of a cardiac plaque mapping data acquisition system in Dr. Zemlin's Cardiothoracic Surgery Research Laboratory. The interface would load and process input signals, calculate data of interest and visualize them on 3D atrial geometry for analysis and understanding of electrical conduction behavior in the atria.

Chapter 1: Introduction

Cardiac arrythmias refers to the disturbance or abnormalities in the normal heart rhythm. The normal heart rhythm (sinus rhythm) begins with a signal is generated in the sinoatrial (SA) node and conducted across the atria of the heart towards the atrioventricular (AV) node. This results in atrial activation and contraction. The signal at the AV node is then conducted through the bundle of His, to the bundle branches, and eventually into the Purkinje fiber, resulting in ventricular activation and contraction. Any disruption in this pathway is called an arrhythmia [1]. The dangers associated with arrythmias are related to the presence of structural heart diseases, e.g. about 50% of heart patients who die of sudden death due to cardiac arrythmia have structural heart disease [2]. Therefore, diagnosis and management of cardiac arrythmias are important in managing the epidemiology of heart disease. Atrial fibrillation (AF) is the most prevalent cardiac arrythmia in humans, with its incidence increasing with increasing age [3] [4]. AF is an arrythmia that happens in the atria of the heart, where abnormalities in electrical signals cause the upper chambers of the heart to contract at a very fast and irregular way (fibrillation) [5]. The irregular atrial contractions cause difficulty in pumping blood out of the atria and increase the risk of blood clots [6]. Therefore, AF is also associated with higher cardiovascular morbidity and mortality, including the increased risk of ischemic stroke and myocardial infarction if AF is left untreated [3]. Due to such complications, AF has become a major public health concern that has severe effects on public health and overall quality of life. Therefore, methods to improve AF diagnosis and management would be helpful in reducing the morbidity and mortality associated with AF. Due to its high prevalence and high association with cardiovascular morbidity and

mortality, there have been many studies directed at understanding the causes and dynamics of AF to develop methods to intervene or mitigate the effect of AF. In fact, AF is among the most studied arrythmia among all heart rhythm disorders, resulting in a major understanding of risk factors and causes of AF as well as the dynamics of AF [4].

However, diagnosis and management of AF are still a major challenge in the field as AF can be asymptomatic at onset, making it difficult to screen and diagnose [3]. Diagnosis of cardiac arrythmia, specifically AF, remains heavily dependent on observation and analysis of the heart's electrical activity to understand the nature of the irregularities [2]. The standard cardiac diagnostic tool is electrocardiogram (ECG), which was developed more than a century ago [7]. As technology continues to develop with improvements in recording facilities and signal processing methods, multiple changes have been made to improve ECG measurements [8]. There have also been major efforts to improve cardiac imaging techniques, including the development of electrocardiographic imaging (ECGI) [9][10].

Cardiac plaque mapping is another cardiac mapping method that is studied in Zemlin's lab. Similar to ECG or ECGI, cardiac plaque mapping studies the electrophysiology of the heart by measuring the cardiac activation and potential using multiple electrodes that are divided into plaques. However, methods such as ECG and ECGI mentioned above measures the far-field potential of the hearts through body surface electrode placement (12-lead for ECG and 224 electrodes for ECGI) and deduce from it either the qualitative activation sequence of the heart (ECG) or the quantitative epicardial potential distribution (ECGI). On the other hand, plaques used in plaque mapping are placed directly on the area of interest in the heart and measure the cardiac signal directly since the plaques carrying the electrodes are in contact with the area of

interest. Therefore, the main advantage of the plaque mapping technique is that more accurate data is obtained from direct measurement. However, the main disadvantage would be much greater invasiveness compared to ECG and ECGI because the electrode needs to be placed directly on the surface of the heart instead of the body surface.

Dr. Zemlin's Cardiothoracic Surgery Research Laboratory is developing a new data acquisition system for cardiac plaque mapping and applying such system to study how mitral regurgitation leads to AF in a canine model. Not only is the canine model similar to a human heart in terms of physical features such as size and weight, but the canine model also resembles the human cardiac electrical behavior [11]. This makes the canine model appropriate for human cardiac electrophysiology. In the context of this study, dog hearts are paced using different pacing modalities (which will be described further in Chapter 2: Methods) to induce arrythmias, specifically AF, and the plaque mapping data of sinus rhythm, paced rhythm, and AF rhythm were collected from the dog hearts as input signal for development of visualization algorithm.

With the development of a new data acquisition system for cardiac plaque mapping in the lab, there is a need for an algorithm that can be used to easily visualize the plaque mapping data to provide a better understanding of the signal collected in relation to the 3-dimensional (3D) geometry. The plaque mapping system consists of three plaques that cover different regions of the atrial surface. This visualization system would also be beneficial in troubleshooting the data acquisition system that the lab is developing as it allows us to identify unexpected signal patterns resulted from an error in the data acquisition system. It will also be helpful as an analysis tool to analyze the electrical conduction pattern of the atria during AF.

The main objective of this thesis is to develop a MATLAB graphical user interface (GUI) that can process and visualize the cardiac plaque mapping signals received from the data acquisition system on the 3D geometry of the atria. To achieve this objective, the study is divided into two parts: signal acquisition/processing and 3D visualization.

The first part of the study focused on loading, processing, and visualizing the data acquired on the 2-Dimensional (2D) geometry of the plaques. This part of the study focuses on understanding the nature of the signal acquired to devise a signal processing plan for the input data. Signal processing will focus on filtering the power line (60Hz) noise from the input signal. There is also a need to remove signals from electrodes that have poor contact with the atria as part of the signal processing process. Once the signal is processed, activation time within a given time window is calculated and visualized, allowing us to further understand the nature of the signal and troubleshoot the current data acquisition system, which helps to push Zemlin's lab's effort in developing a new plaque mapping data acquisition system.

Once data have been loaded and processed on the level of the 2D plaques, the second part of the study focuses on projecting data from the 2D plaques onto the 3D atrial geometry. The projection is achieved by determining for each plaque a transformation (a combination of translation and rotation) that maps the 3D atrial geometry onto the 2D geometry in a way that reflects the actual positioning of the plaque on the atrium. Vertical projection of the atrial vertex mesh points and interpolation of the electrode signal values (voltages or activation time) enables mapping of the plaque data onto the 3D atrial geometry. Displaying the data in 3D integrates the data from the different plaques and puts them into correct spatial relation and in this way facilitates their interpretation. The data that are displayed in 3D could be the actual epicardial

voltage or derived data such as activation maps or action potential duration maps. An intuitive and accurate 3D representation of electrophysiological data greatly helps in the accurate assessment of the dynamics of arrythmias (including AF) pattern, which is the first step to combat such cardiac complications.

Chapter 2: Methods

2.1 Signal Acquisition and Processing

2.1.1 Overview of Electrode Plaques and Pacing

Epicardial electrodes are distributed over three plaques with each placed in a different location on the dog's heart, specifically the left posterior atrium (LP) plaque, the right posterior atrium (RP) plaque, and the biatrial plaque. The name of plaques is named according to their location on the heart: LP plaque, RP plaque and biatrial plaque. The images of the three plaques with electrodes are shown in Figure 2.1. The relative position of the plaques on the 3D atria is shown in Figure 2.2

A variety of methods are used to pace the dog hearts to induce arrythmia, specifically AF, including 300 ms pacing, s1-s2 pacing, or burst pacing. 300 ms pacing pace the dog hearts at a constant basic cycle length (BCL) of 300 ms. s1-s2 pacing includes pacing the hearts 8 pulses at a constant BCL, similar to that performed in 300 ms pacing, followed by an extra pulse at a different interval, typically a shorter time. Burst pacing pace the heart with rapid pulses at constant rate. In the context of the datasets used in developing the algorithm for the MATLAB interface, 300 ms pacing was applied at the right atrial appendage (RAA) with approximately 2 mA. The pacing beats are watched closely as the signals at the electrode are recorded by the recording system.

(a)

(b)

(c)

Figure 2.1 Images of (a) Left Posterior Atrial Plaque (b) Right Posterior Atrial Plaque (c) Biatrial Plaque with electrodes connected to the Intan System. Rulers are placed side-by-side for scale.

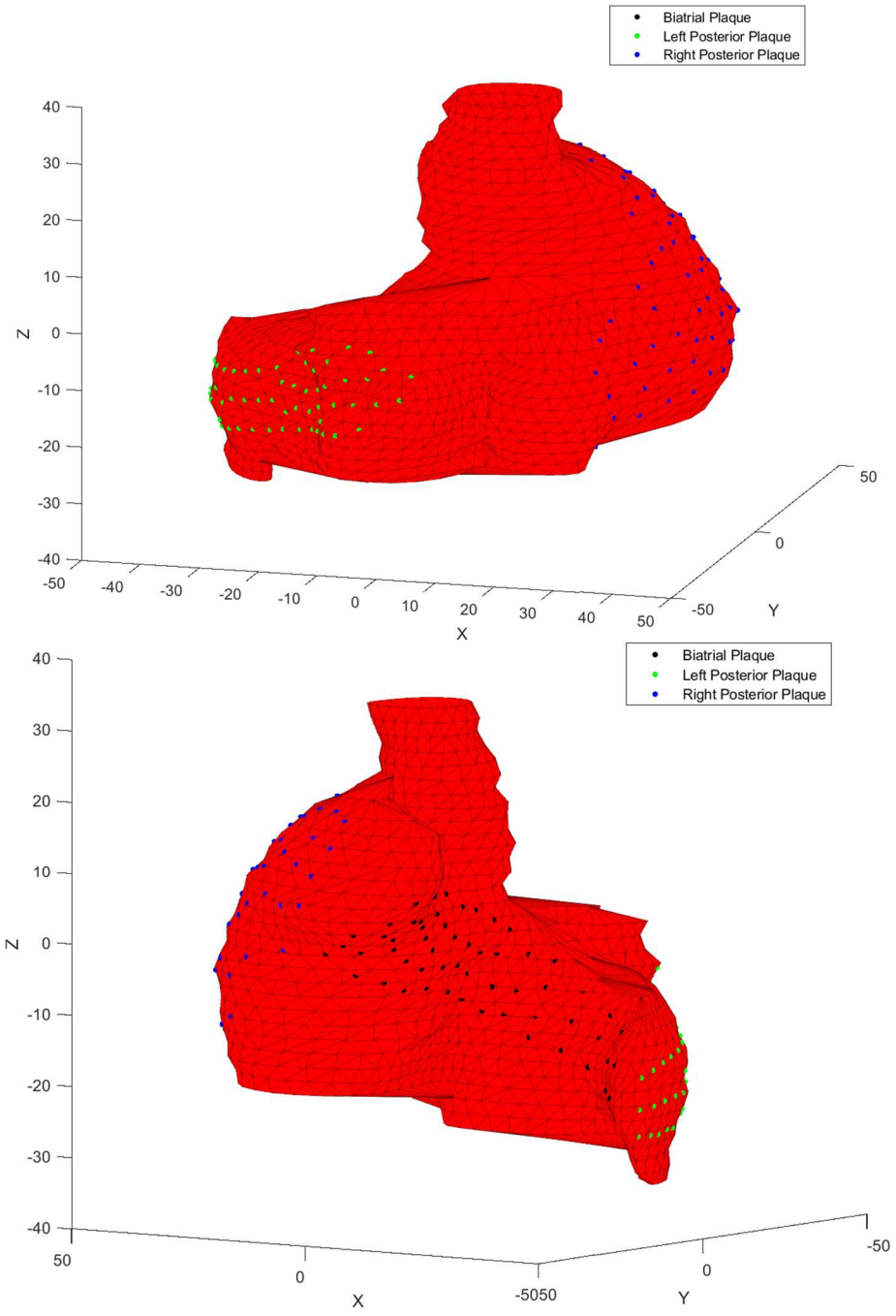

Figure 2.2 Two views of the 3D rendering of the atria and the plaque showing the relative position of the three plaques on the atria (black: biatrial, green: LP, blue: RP)

2.1.1 Recording System

Electrical signals acquired from the electrode plaque placed on the heart atria are recorded using the RHD2000 system (Intan Technologies, Los Angeles, CA), which is designed to allow the recording of biopotential signals from multiple low-noise amplifier channels.

The plaque mapping system utilized in the Zemlin lab uses a total of 224 channels from the Intan Recording System for data collection. Channels are divided into patches labeled with letters A-G, with each patch containing 32 channels labeled numerically from 0 to 31. The channel identifiers composed of a letter and a number from 0 to 31 (e.g., “A26”) will be referred to as the Intan key in this thesis.

Intan Technologies provides open-source MATLAB code to import the .rhd output file from the Intan recording system into the MATLAB workspace. This MATLAB RHD reader function is utilized to import the collected electrode signals into MATLAB for further processing and visualization.

2.1.2 Signal Processing and Activation Time Calculation

Signal Processing

Once electrode signals are imported to MATLAB, Bandstop Filter is applied to the signal to remove 60 Hz noise from the input signal. A 60 Hz Bandstop Filter is a Butterworth Bandstop filter developed using the Filter Designer Graphic User Interface (GUI) in Signal Processing Toolbox from MATLAB, with a sampling frequency of 2000 Hz, lower cut-off frequency at 59 Hz and higher cut-off frequency at 61 Hz (Figure 2.3).

```
% Butterworth Bandstop filter designed using FDESIGN.BANDSTOP.

% All frequency values are in Hz.
Fs = 2000;  % Sampling Frequency

N   = 10;    % Order
Fc1 = 59;  % First Cutoff Frequency
Fc2 = 61;  % Second Cutoff Frequency
```

Figure 2.3 Setting details of the 60 Hz Bandstop Filter used.

A 60 Hz Bandstop filter is applied to the signals via a MATLAB function to ensure that the filter applied to our signal is zero phase as phase shift is not desired during filtering. The MATLAB function takes in the filter and the signal as input, applies the filter in the forward direction, reverses the filtered data, reapplies the filter, and then reverses the filter data back before returning the filtered data as function output.

Activation Time Calculation

An activation time map is a compact and informative way to describe how excitation propagates over the heart. Activation maps look at a single activation time that occurs in a specified time window, so our software needs the ability to select a time window before activation time calculation. A window of typical signal recorded showing a single activation is shown in Figure 2.4 (all channels are superimposed). In each activation window, there are two regularly paced signals recorded: an atrial signal followed by a ventricular signal. The atrial signal has a wider distribution over different electrode locations as the atria points are activated at different times with slight delay. The ventricular activation is more simultaneous, reflecting the short QRS complex. Since we are only interested in atrial activation for this study, the

activation time window can be manually identified from the plot of filtered data over time by selecting the starting and ending time of the more widely distributed signal.

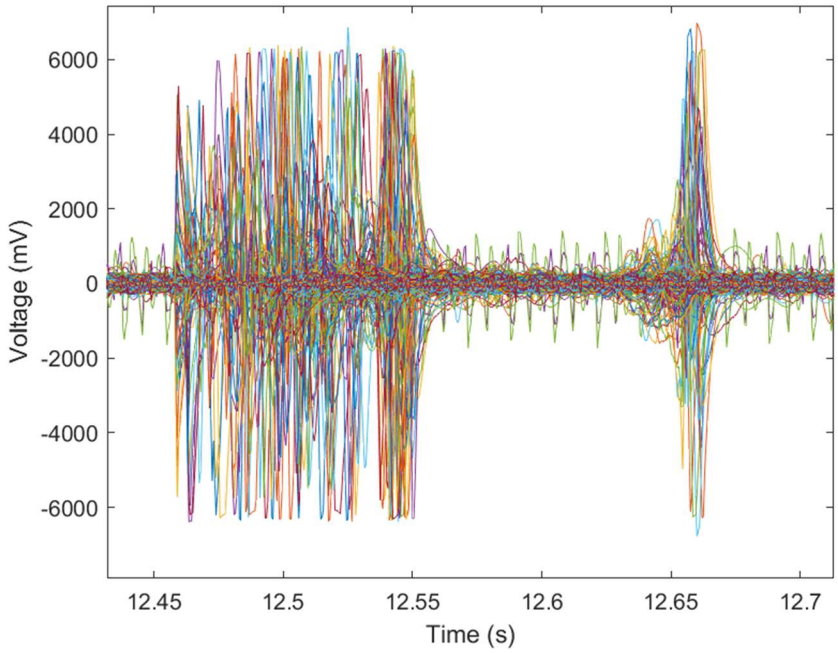

Figure 2.4 Portion of the signal showing a pacing signal that is simultaneously across channels followed by the atrial signal that is more spread out reflecting the atrial electrical conduction pattern.

Once the activation window is identified, the activation time of each channel in this window can be calculated. There are several methods to identify the activation time from the signal, including determining the point of maximum negative slope, or the midpoint between absolute maximum and absolute minimum voltage or the point of absolute maximum voltage as activation time. The point of absolute maximum voltage is chosen as the method for identifying the activation time in this study as it would be more robust compared to the other methods. For ease of comparison and visualization, activation time (rounded to the nearest ms) is calculated relative to the start of the chosen time window using Equation 2.1.

*Relative activation time = round ((activation time – window start time) * 1000)* (Equation 2.1)

2.1.3 Interpolation of Data Values

Interpolation is used to approximate atrial values based on nearby electrodes value (i.e., activation time or voltage) due to its accuracy in approximating the value of points within a known boundary. The MATLAB function *scatteredInterpolant (x, y, v)* is used to create an interpolant that fits a surface of the form $v = F(x, y)$ with (x, y) be the coordinates of the electrode points and v as the value associated with the point (x, y). The function F = *scatteredInterpolant (x, y, v)* will then be used to determine the value of the chosen atrial points by doing $v_A = F(x_A, y_A)$ where (x_A, y_A) is the coordinates of the projected atria points and v_A is the calculated value associated with the point (x_A, y_A). For better accuracy, the local *scatteredInterpolant* F function is determined for every atrial point. A set of nearby electrodes points are chosen to perform triangulation-based interpolation via *scatteredInterpolant* function and the value for the corresponding atria point is calculated. The set of nearby electrode points is determined by setting a threshold to the distance between the atria points and the electrode points. The threshold is calculated as *threshold = k * min(distance between electrodes)* where k is a hyperparameter. In this study, k is set to 8 based on trial results to ensure that for every atrial point, enough electrode points are chosen for triangulation.

2.2 Signal Visualization

The plaques with the recording electrodes are two-dimensional. As we described above, data collected from the individual electrodes can be filtered, processed, and interpolated on the level of a plaque. It is desirable, however, to project the data from all plaques onto a 3D atrial

geometry, for a better appreciation of the spatial information provided from all the data of the plaques in an integrated way. We are currently using a specific idealized atrial geometry for visualizing the data collected from different animals. For accurate visualization, it is important to specify the position of the individual plaques in the atrial geometry before projecting the data. Once the correspondence between plaque coordinates and 3D mesh points is established, the data to be visualized on the 3D mesh can be obtained via this correspondence and interpolation in 2D. Dr. Zemlin's lab is moving towards reconstructing the individual atrial geometries for each animal, and the same approach will still be applicable in this situation.

2.2.1 3D Geometry Rotation of Plaques and Atrial Geometry

To allow for accurate projection of atria vertices onto the plaque plane, the plaque plane and the atria geometry need to be positioned such that the plaque is attached to the atria geometry at the position at which it was placed during the experiment (i.e., LP, RP, biatria). This requires previous knowledge of anchor points on the atria geometry that corresponds to known 2D plaque electrodes. For this study, two atrial anchor points (labeled A_a and B_a) are chosen to match two 2D plaque electrodes (labeled A_p and B_p respectively). For further experiments and study, these anchor points - plaque electrodes pair will be determined during signal acquisition procedure in the OR by the surgeons.

The match between plaques and atrial geometry can be achieved by either moving the plaques to match the atrium or vice versa. For simplicity, we consider the plaques sequentially and position the plaque in the xy-plane in each case.

To simplify the later transformations, the 2D plaque is first translated such that point A_p is set to the origin (0, 0, 0). The plaque subsequently rotated in the xy-plane around point A_p such that A_pB_p aligns with the x-axis; therefore, the angle of rotation would be the angle θ between vector A_pB_p and the x-axis (Figure 2.5), which can be calculated using Equation 2.2

$$\theta = \tan^{-1}\frac{B_y}{B_x} \qquad \text{(Equation 2.2)}$$

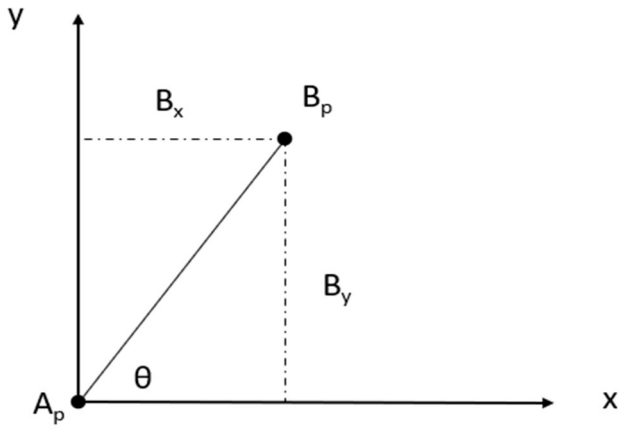

Figure 2.5 Drawing showing the angle of rotation and the geometry for deducing Equation 2.2. B_p is the point to be rotated to the x-axis. B_x and B_y are the distance between B_p and the x-axis and y-axis respectively.

Given this angle of rotation, the rotation matrix can be defined as Equation 2.3. However, it is important to note that this rotation matrix only applies to the counterclockwise angle between vector A_pB_p and the x-axis, which can only be visually determined. Visual determination cannot be applied to the software; therefore, a method is necessary to ensure that the right angle is chosen such that point B_p is rotated onto the x-axis. Assuming point B_p is rotated onto the x-axis, its y-coordinate should be zero. Therefore, to decide between the positive and negative θ values to be used for formation of the rotation matrix, the y-coordinate of point B_p after rotation using both θ values is examined. The θ value that gives a y-coordinate of zero will be used to form the rotation matrix using Equation 2.3

$$R = \begin{bmatrix} \cos\theta & -\sin\theta \\ \sin\theta & \cos\theta \end{bmatrix} \quad \text{(Equation 2.3)}$$

Once the rotation matrix is determined, the plaque points undergo transformation that includes subtracting the coordinate of A_p from the coordinate of the plaque points (translation) followed by multiplying the rotation matrix R_p with the plaque point coordinate (rotation). The transformation of plaque point (x_i, y_i) is demonstrated mathematically in Equation 2.4

$$\begin{bmatrix} x_i \\ y_i \end{bmatrix} = R_p \begin{bmatrix} x_i - A_x \\ y_i - A_y \end{bmatrix} \quad \text{(Equation 2.3)}$$

Once the plaque is positioned such that A_pB_p is aligned with the x-axis and A_p is at the origin, the atria mesh will undergo transformation to position the atria in the correct relative position to the plaque. Aligning the atrial geometry with the plaque requires scaling the 3D atrial geometry such that the distance A_pB_p between two anchor points is equal to the distance A_aB_a between the two plaque points. To maintain the shape of the atria geometry, all the atrial vertices are uniformly scaled using the same scaling factor calculated using Equation 2.4 where *norm (vector)* function calculates the vector norm of the input vector.

$$Scaling\ factor = \frac{norm(B_p - A_p)}{norm(B_a - A_a)} \quad \text{(Equation 2.4)}$$

Once the geometry is scaled to match the two distances, the atrial vertices need to be translated such that point A_a on the atria matches point A_p on the plaque (or the origin) and rotated such that point B_a on the atria matches point B_p on the plaque. The rotation matrix is determined using Rodrigues' rotation formula for 3D rotation (Equation 2.5) where k is a unit

vector describing the axis of rotation. For any two non-zero vector **a** and **b** that defines the plane of rotation, θ is the angle measured away from **a** and towards **b**, and I is a 3x3 identity matrix:

$$k = \frac{\boldsymbol{a} \times \boldsymbol{b}}{|\boldsymbol{a} \times \boldsymbol{b}|}$$

$$K = \begin{bmatrix} 0 & -k_z & k_y \\ k_z & 0 & -k_x \\ -k_y & k_x & 0 \end{bmatrix}$$

$$R_a = I + (\sin\theta)K + (1 - \cos\theta)K^2 \qquad \text{(Equation 2.5)}$$

To apply Equation 2.5 to our geometry, vector **a** is point B_p and vector **b** is point B_a. Since the plaque is aligned to xy-plane, the z-coordinates of all plaque points (including A_p and B_p) are zero. The angle θ between B_p and B_a is determined using Equation 2.6 and the rotation matrix is defined using Equation 2.5

$$\theta = \cos^{-1}\frac{B_p \cdot B_a}{|B_p||B_a|} \qquad \text{(Equation 2.6)}$$

Once again, to ensure that the right angle is chosen for rotation matrix formation, the coordination for B_a is calculated using both positive and negative θ. The θ value that makes B_a equal to B_p will be chosen.

Once the rotation matrix is calculated, the atrial vertices all undergo a transformation that includes subtracting the coordinate of A_p from the coordinate of the atria vertices (translation) followed by multiplying by the scaling factor, followed by multiplying the rotation matrix R_a with the vertex coordinate (rotation). The transformation of atria vertex (x_i, y_i, z_i) is demonstrated mathematically in Equation 2.7

$$\begin{bmatrix} x_i \\ y_i \\ z_i \end{bmatrix} = R_a \left(scaling\ factor * \begin{bmatrix} x_i - A_x \\ y_i - A_y \\ z_i - A_z \end{bmatrix} \right) \qquad \text{(Equation 2.3)}$$

Once the above transformation is performed, anchor points and electrode points should be checked to ensure that they match each other (i.e., point A_p matches A_a and point B_p matches B_a) before proceeding with the next step. After the pairs of anchor – electrode points are aligned, the atria geometry undergoes the last rotation that rotates the atria geometry around the vector AB (or x-axis) to reposition the plaque for projection. Since this is a rotation around the x-axis, the rotation matrix is defined as Equation 2.3 where θ is the angle of rotation. This angle of rotation will be determined by the user to visually ensure that the plaque matches the atrial geometry as well as possible.

2.2.2 Projection of Atria Vertices onto Plaque Plane

Once the plaque is positioned to match its position relative to the atria during the experiment, the atria points are projected onto the plaque plane. Atrial points will typically not coincide with measurement points on the plaque, but the data that are being visualized can be interpolated on the 2D plaque, so the correct data value for the mesh vertex can be determined. It is important to note that the signals collected are bipolar signals; therefore, the signal does not correspond to the electrode locations but corresponds to the midpoints between the electrodes (measurement locations). The plaque point coordinates recorded in this study are the measurement locations. As mentioned previously, the interpolation needs to be done on the 2D plaque plane, which makes it necessary for the projection of atria points onto the plaque plane (or xy-plane). Since this is a projection onto the xy-plane, the z-coordinates of the atrial points

are set to zero to generate the projected atrial points. To prevent atrial points outside the local neighborhood of the plaque from getting assigned interpolated values, a distance threshold is set to eliminate points from the opposite side of the heart. Since interpolation can only be performed with points within the plaque boundary, only atrial mesh points that project into the plaque area will be assigned values. The boundary of the plaques is determined from the electrode coordinates using the *boundary (x, y)* MATLAB function which determines the boundary of a set of points in 2D given their x, y coordinates. To determine if the projected atrial points fall within the boundary, *inpolygon (xq, yq, xv, yv)* MATLAB function is used. This function takes in points (xv, yv) that determine the boundary of the area of interest and the set of query points (xq, yq) and returns a logical matrix indicating if the query points fall within the area of interest. With these two MATLAB functions, we can identify the atrial points that will be assigned data values via projection and interpolation. Once the atrial points are projected, interpolation function derived above can be used to obtain the atrial value.

2.2.3 Visualization of Interpolated Atrial Value

The transformation, projection, and interpolation process are repeated for all three electrode plaques and the interpolated atrial values are recorded. Using the recorded atrial value, *trisurf (T, x, y, z, c)* function in MATLAB is used to create the 3D triangular surface defined by the points in atria triangular face T and atrial points (x, y, z). Atrial value c will determine the color of the plot. Points that do not have an interpolated atrial value will be masked (i.e., assigned the color black). Voltage map video is also generated using *VideoWriter* function from MATLAB that allows combining figures as frames to create a video. The frame rate of the video is set to 5 frames per second (fps).

Chapter 3: Results

The results presented below are for a single data set that is measured for external pacing at the right atrial appendage (RAA) with a basic cycle length of 300 ms.

3.1 Data Processing

Figure 3.1 shows the effect of the filter on the acquired signal as a lot of the noise that cover the signal in Figure 3.1 (a) has been removed to display more meaningful signals in Figure 3.1 (b)

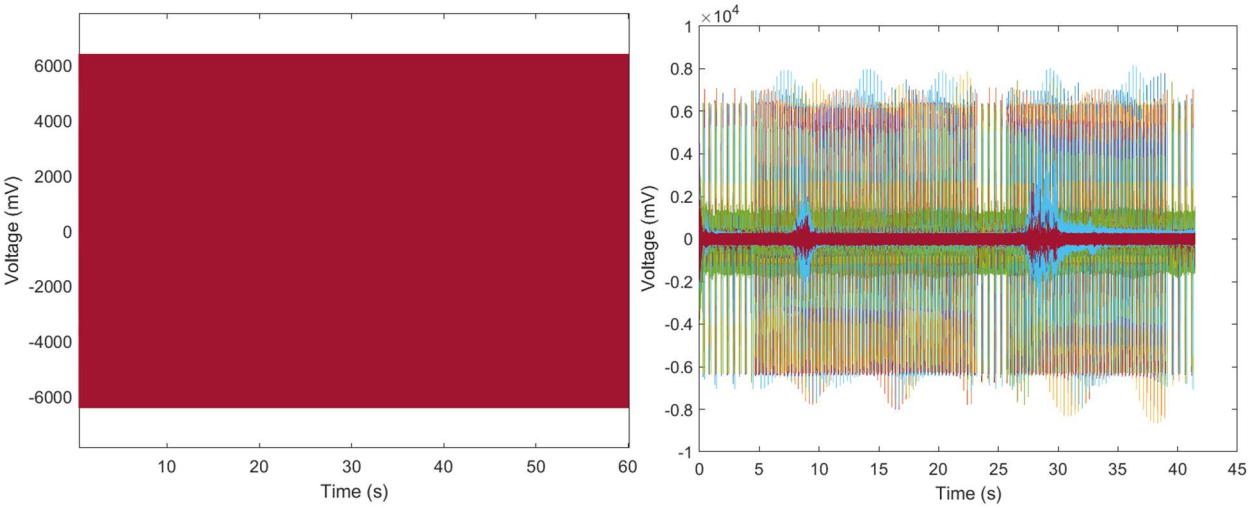

(a) (b)

Figure 3.1 Superimposed epicardial potentials from all electrode channels (a) before and (b) after applying 60 Hz Bandstop Filter.

A zoomed-in portion of the filtered signal (Figure 3.2) shows clear periodicity, reflecting the fact that we are periodically stimulating (with a period of 300 ms). The atrial and ventricular activation signal behavior described in the previous chapter is also clearly seen here where the

atrial activation signal is more widely distributed followed by a more simultaneous ventricular activation signal.

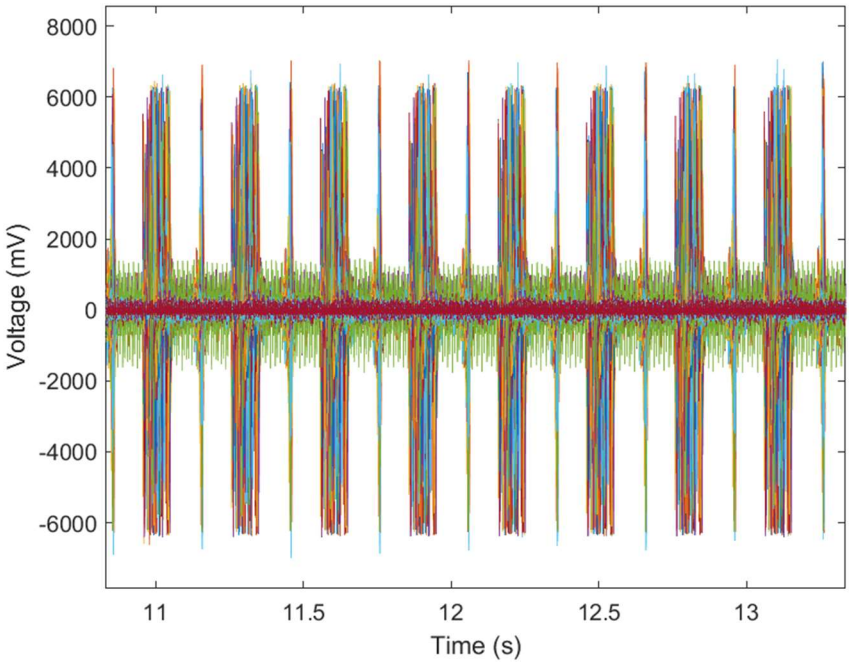

Figure 3.2 A portion of the filtered signal

Figure 3.3 shows a window of a single activation, which is 12.453 – 12.563 seconds. This activation window is specific to this signal and is representative of only one of the many activations that were recorded. Once the activation window is determined, the activation time for all the signals within that period is determined using Equation 2.1. Figure 3.4 shows an example of an activation time relative to the activation window start time. There is a small discrepancy seen in Figure 3.4 because of rounding the nearest millisecond.

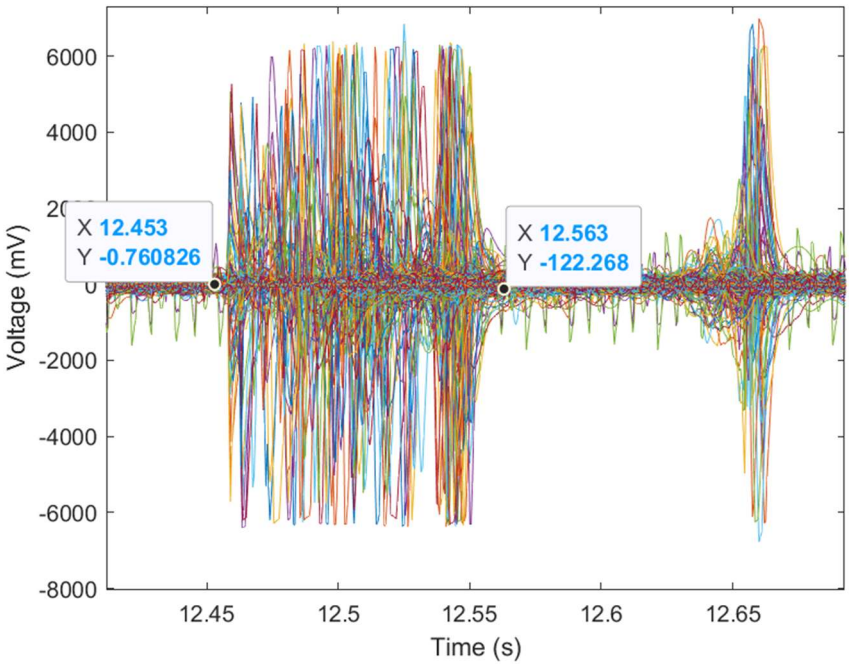

Figure 3.3 A portion of the filtered signal indicating the expected spike behavior. Indicated points identify the start and end point of the activation window of interest.

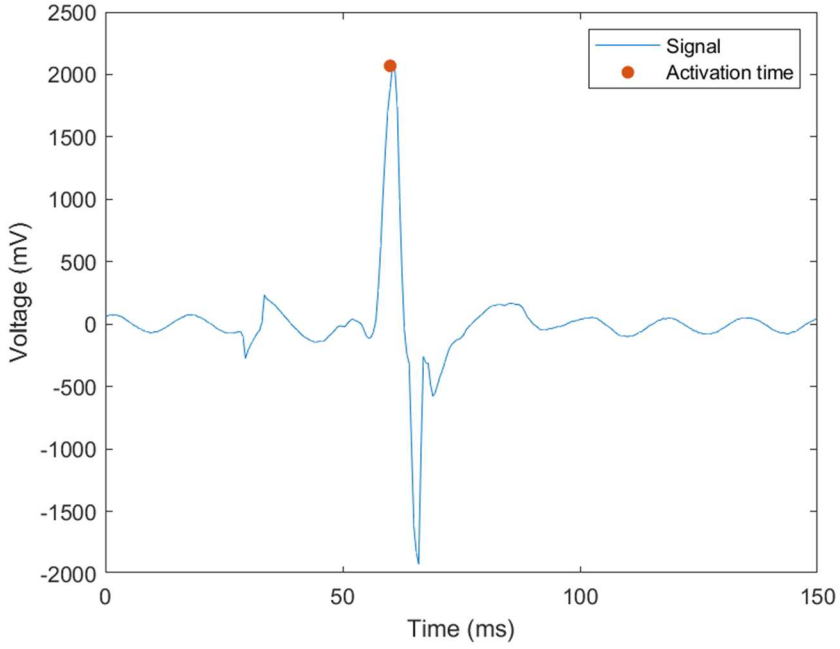

Figure 3.4 Activation time (red point) is defined at the time when absolute maximum voltage is achieved.

3.2 3D Visualization

3.2.1 Geometry

The 2D geometry of the plaques are shown in Figure 3.5 (biatrial), 3.6 (LP) and 3.7 (RP). This geometry was collected during the signal processing procedure in the OR by the surgeons, with the points being the measurement location of the bipolar signals (i.e., the midpoint between two electrodes). This geometry will be used to visualize the distribution as well as interpolate the value of interest, including the activation time that was calculated earlier. Other measurable values can also be used as values for interpolation such as voltage, phase difference, etc. However, in this study, only activation time and voltage are studied. For this portion of the thesis, activation time will be used as the value of interest.

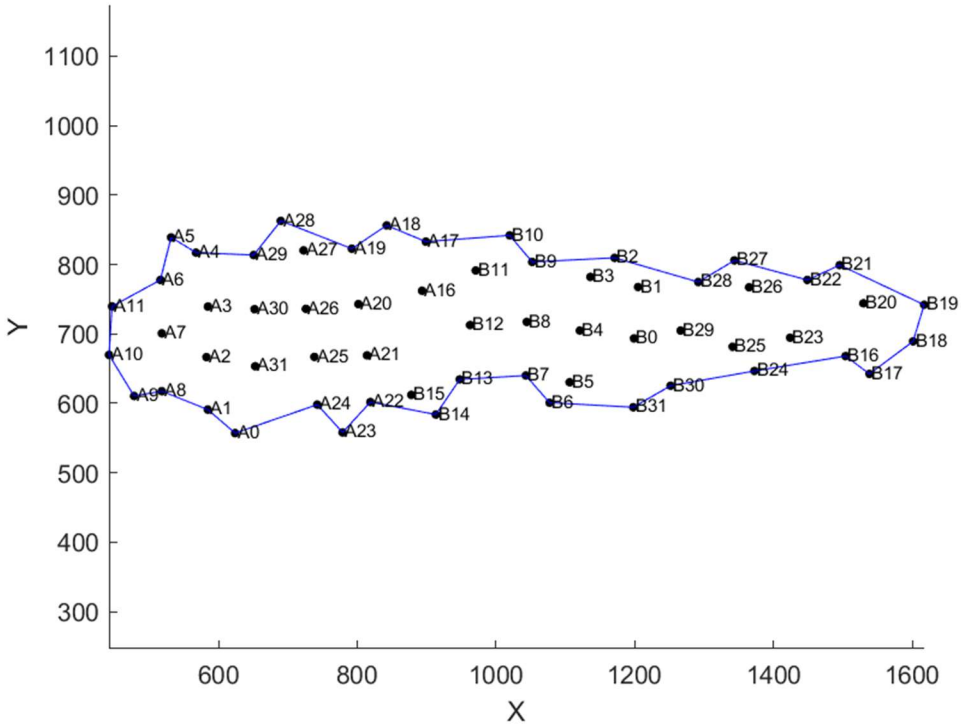

Figure 3.5 Geometry of the biatrial plaque

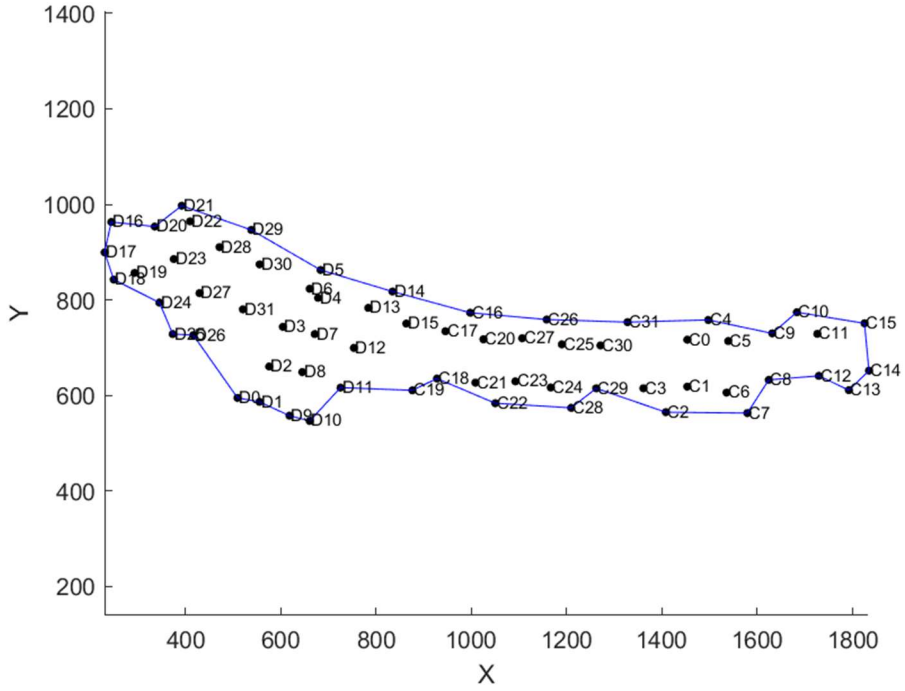

Figure 3.6 Geometry of the LP plaque

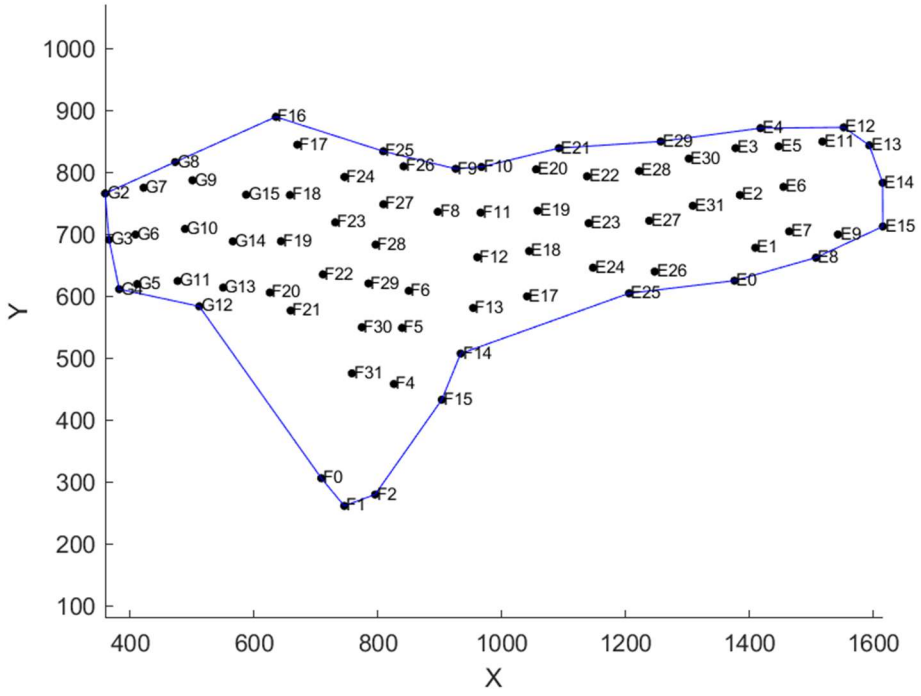

Figure 3.7 Geometry of the LP plaque

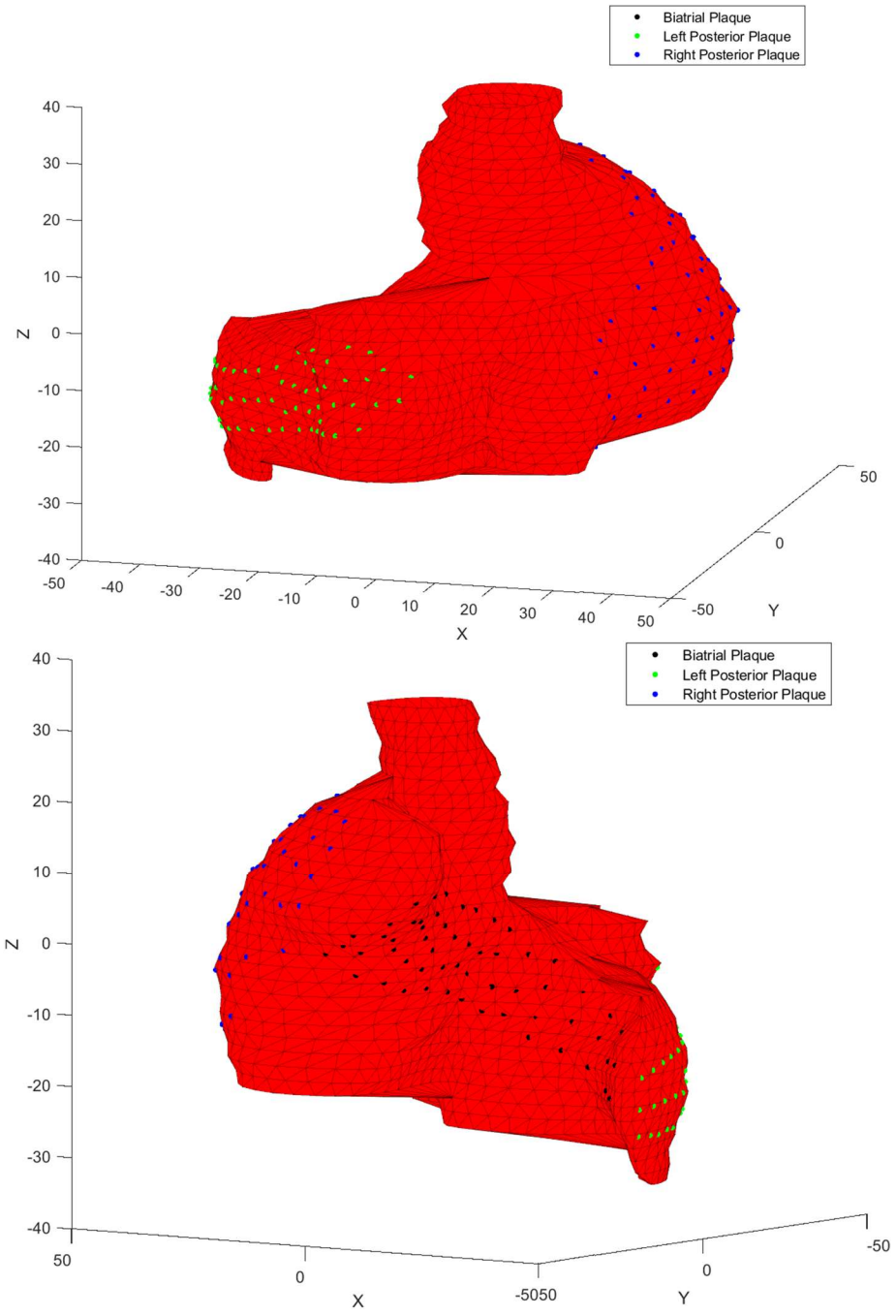

Figure 3.8 Two views of the 3D geometry of the atria and the plaque showing the relative position of the three plaques on the atria (black: biatrial, green: LP, blue: RP)

The reference 3D atria and electrode geometry are shown in Figure 3.8. This geometry will be used for 3D visualization of the value of interest (i.e., activation time). It is important to note that the plaque positions shown in Figure 3.8 are only approximate and shown as a general

illustration. In reality, the atria can vastly vary in size due to the medical condition that is studied (mitral regurgitation in this context). With mitral regurgitation, the left atrial volume can increase by a factor of five. The change in atrial size between different hearts also affects the contact between the plaque and the atria, which will be explored in the later part of this thesis.

The pair of anchor points and plaque points are presented in Table 1. These values are approximate for this study. However, moving forwards, this information will be obtained and recorded in the OR by the surgeons during the signal recording procedure.

Table 1: Pair of anchor point – plaque points for all three plaques

Plaque	Plaque Intan Number		Atrial Anchor Point Index	
Biatrial	A_p	A31	A_a	997
	B_p	B0	B_a	707
Left Posterior	A_p	D31	A_a	535
	B_p	C1	B_a	603
Right Posterior	A_p	E1	A_a	728
	B_p	G14	B_a	1233

3.2.2 Interpolation

Interpolation is done on the 2D plaque using activation time as the value for interpolation. The distribution of activation time for three plaques is shown in Figure 3.9 (biatrial), 3.10 (LP), and 3.11 (RP).

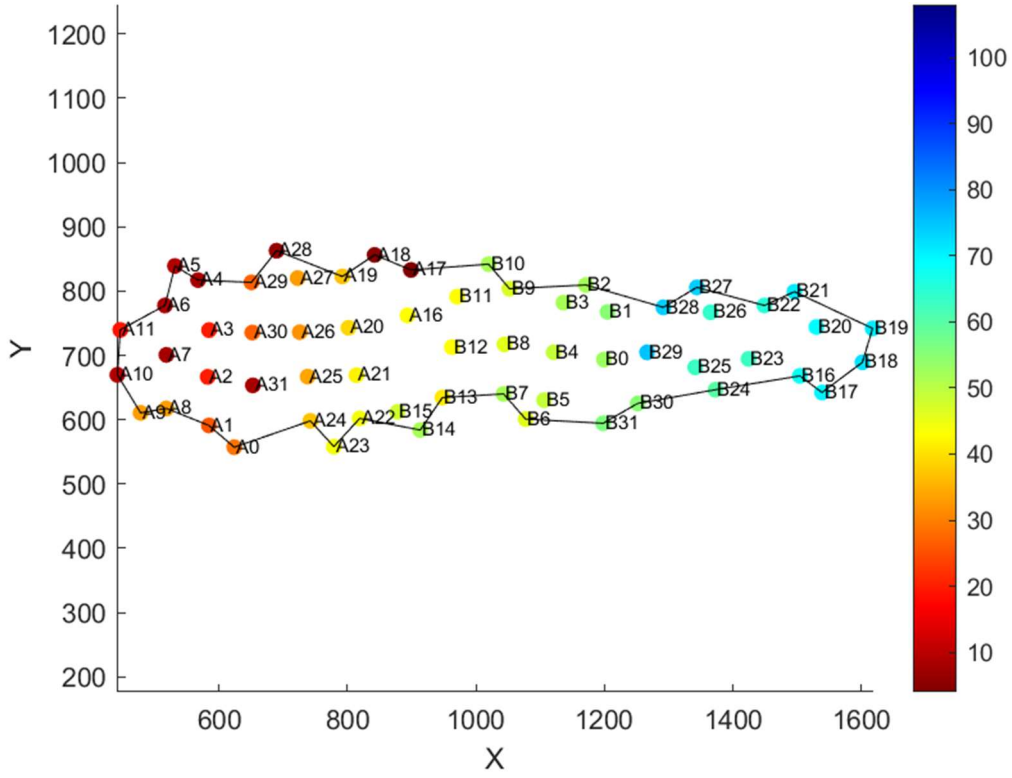

Figure 3.9 Activation time map for the biatrial plaque

Figure 3.10 (a) and 3.11 (a) shows areas of activation time where the activation time is not consistent with the rest of the plaque. Specifically, there is early activation in the area from C10 – C15 for LP plaque (Figure 3.10a), and an area on the upper right of the RP plaque (Figure 3.11a).

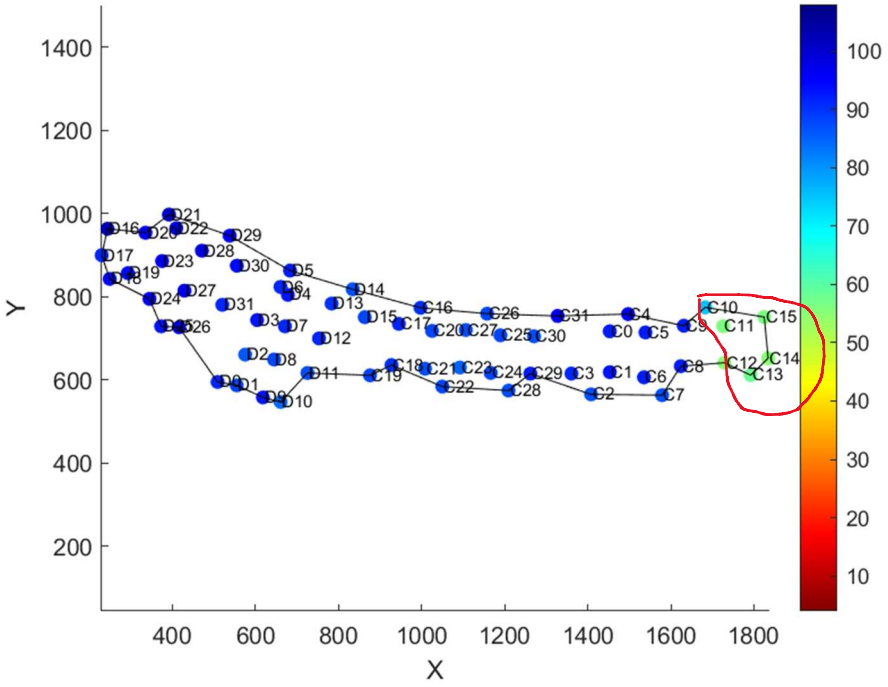

(a)

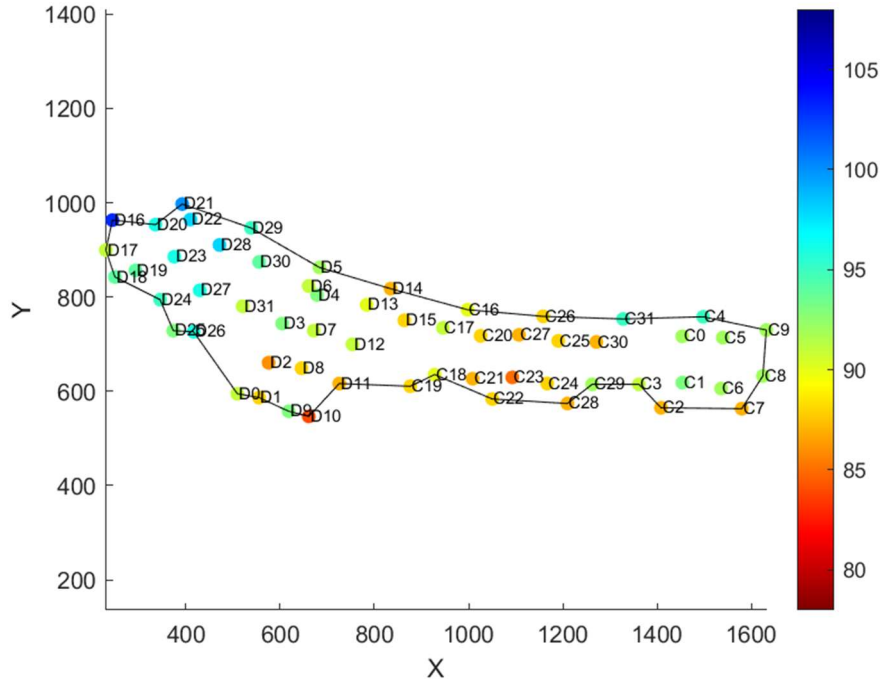

(b)

Figure 3.10 (a) Distribution of activation time in LP plaque. Area circled in red shows an area in which plaque electrodes did not have contact with cardiac tissue. (b) Distribution of activation time in LP plaque with selected electrodes removed. The color bar scale is adjusted to better see the difference in activation time within the LP plaque since there is little difference in the activation time in the LP atria.

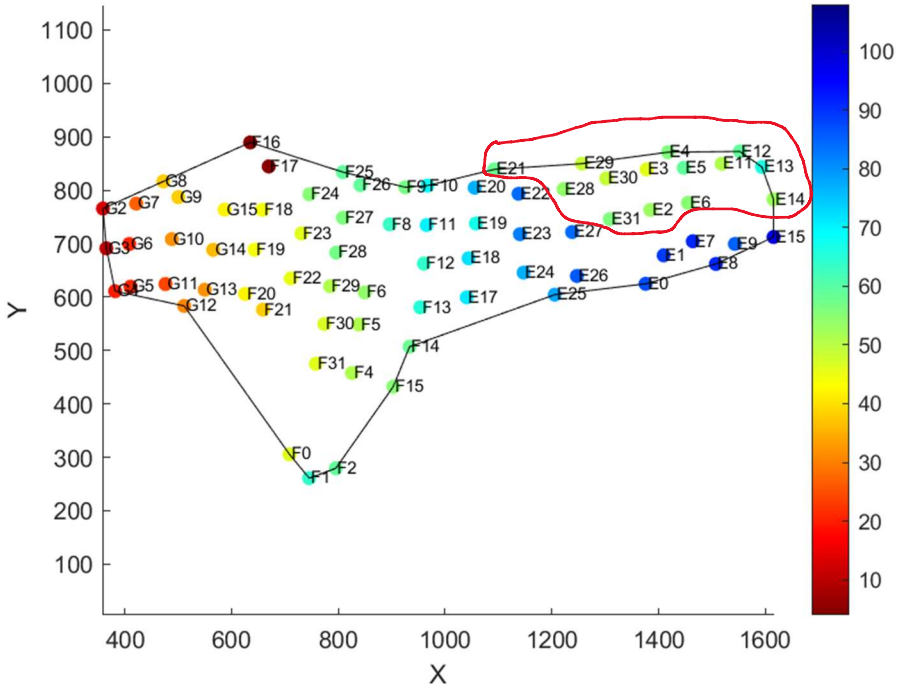

(a)

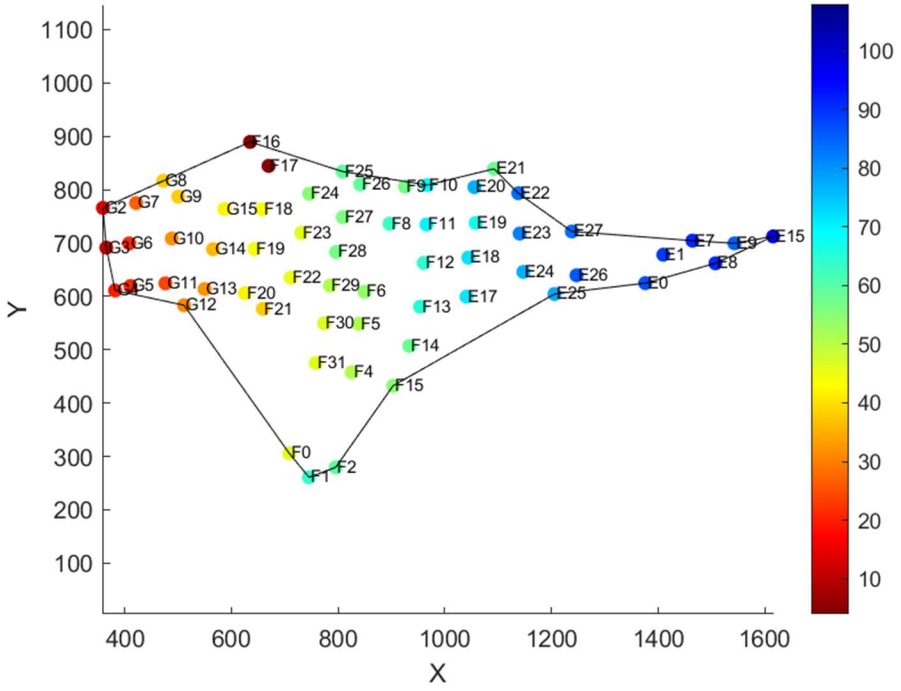

(b)

Figure 3.11 (a) Distribution of activation time in RP plaque. Area circled in red shows an area in which electrodes were not in contact with cardiac tissue. (b) Distribution of activation time in RP plaque with selected electrodes removed.

The possible reason for this inconsistency is inspected by looking at the individual signals recorded at these electrodes. The signal of one of the electrodes for each of the plaque investigated is shown in Figure 3.12 (C11 for LP and E30 for RP), showing that there is no atrial activation peak recorded at this position and only ventricular activation signal is recorded. This behavior is representative of all the points' area circled red in Figure 3.10 (a) and 3.11 (a). This suggests that these electrodes did not detect atrial activation signals. This is relevant to the problem in size variety between atria discussed earlier. Since the heart differs in size due to different medical conditions, part of the plaques (especially LP and RP) has to be placed off the atria and into the ventricle. This results in this portion of the plaques not detecting the atrial signal. Therefore, for the purpose of this study, these electrodes will be removed from the plaques (Figure 3.10 – 3.11 b).

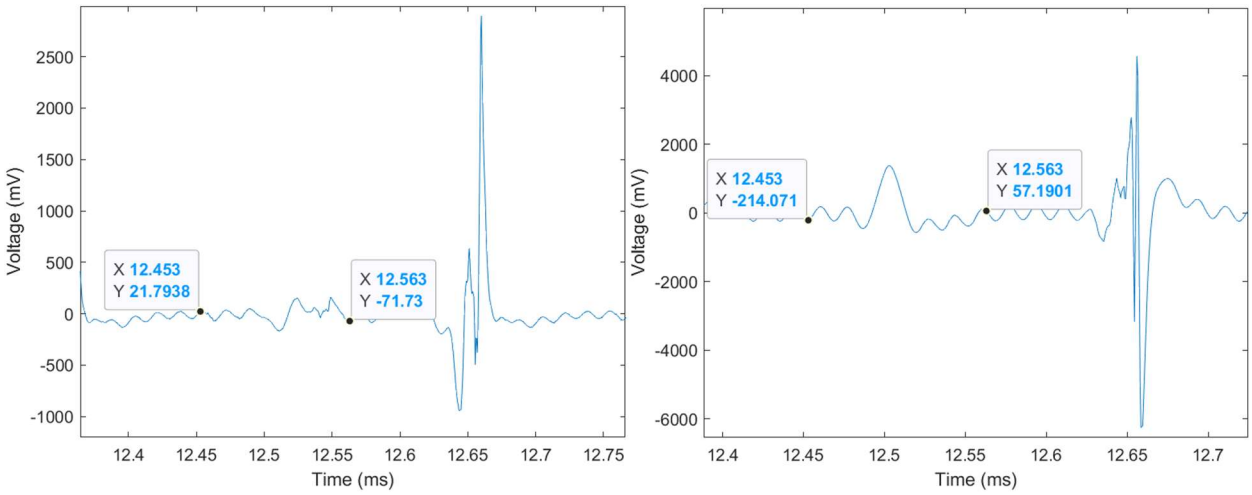

(a) (b)

Figure 3.12 Portion of the signal for (a) Electrode C11 in LP and (b) Electrode E30 in RP. No atrial activation is seen in the activation window of interested identified earlier (indicated by the points shown)

3.2.3 Rotation

Since the procedure for deducing the rotation of the plaque and atria mesh is similar in all three plaques, the result of the rotation of the biatrial plaque is shown as representative of all three plaques.

Plaque Transformation

Figure 3.13 shows the biatrial plaque after translation with the red crosses indicating the plaque points which correspond to the chosen atrial anchor points (Table 1). The translation successfully moves the plaques such that point A_p (A31) is now at the origin.

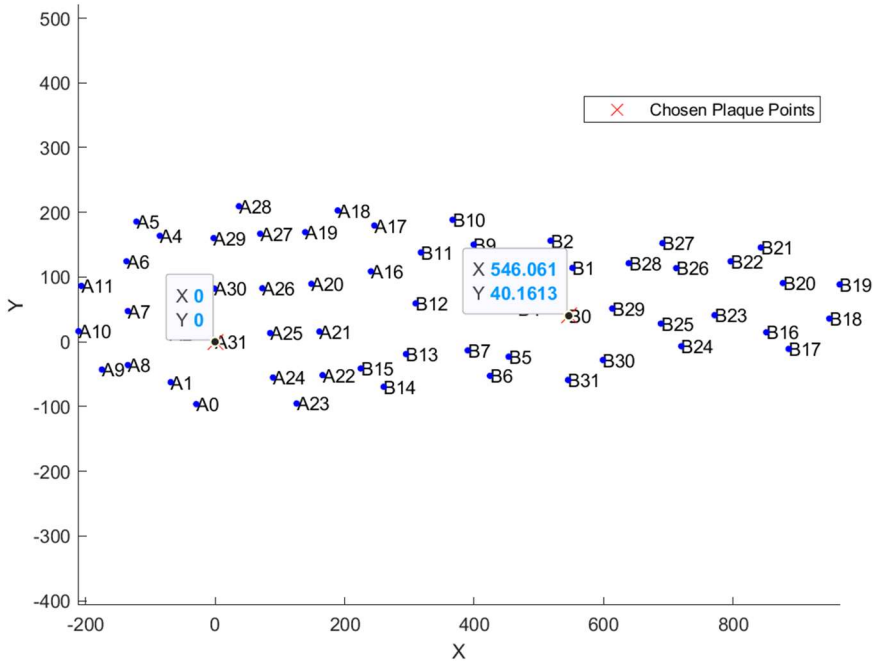

Figure 3.13: Plaque position after translation. Red crosses indicated the anchor points. The plaque has been translated such that point A_p is translated to the origin (coordinate shown)

Figure 3.14 shows the plaque after the rotation that aligns vector A_pB_p with the x-axis. Comparing Figure 3.13 and 3.14 shows that the coordinate of point B_p has become zero after the

rotation matrix is applied, verifying that the rotation matrix was calculated correctly, and the rotation of the plaque to align vector A_pB_p with the x-axis is as expected. There is no distortion in the shape of the plaque after the transformation, verifying that there is no error in the transformation.

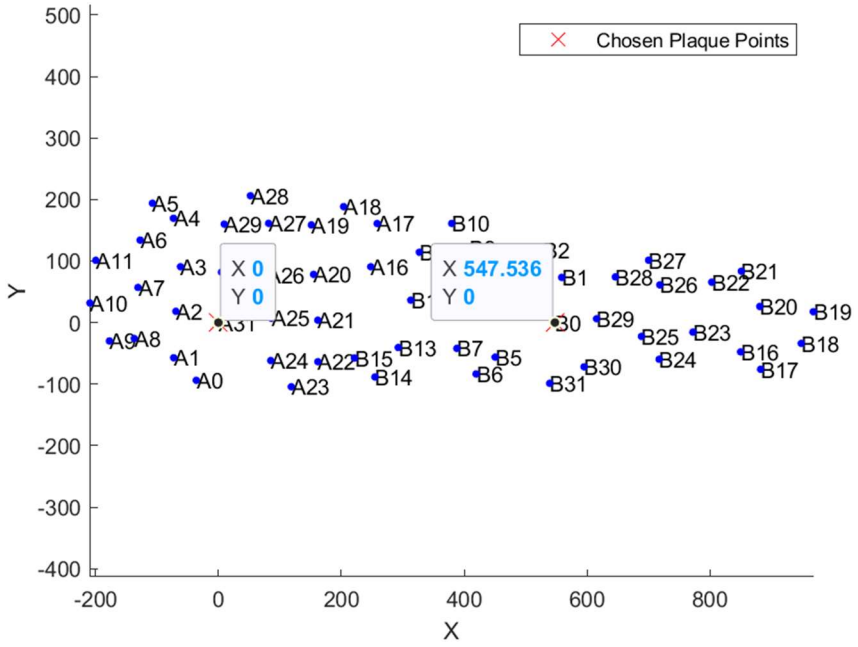

Figure 3.14: Translated plaque after rotation. Red crosses indicated the anchor points. Plaque has been rotated such that vector A_pB_p align with the x-axis, indicated by y-coordinate of point B_p being set to 0 (coordinate shown)

Atria Transformation

Atrial mesh undergoes transformation that includes translation to match point A_a to A_p, scaling to match distance A_aB_a to A_pB_p, and rotation to match point B_a to B_p. The rotation matrix was determined using Equation 2.5 and the resulting atria geometry with biatrial plaque is shown in Figure 3.15. From Figure 3.15, we see that the two atrial anchor points match the two corresponding plaque points and there are no distortion in the shape of the mesh, indicating that

the transformation is successful in positioning the plaque to the atria using the two anchor points. However, it is clear that the plaque is not aligned at the right angle with respect to the atria. This behavior is expected, which is why a third rotation around the x-axis is designed to align the plaque at an accurate angle relative to the atria before performing projection and interpolation.

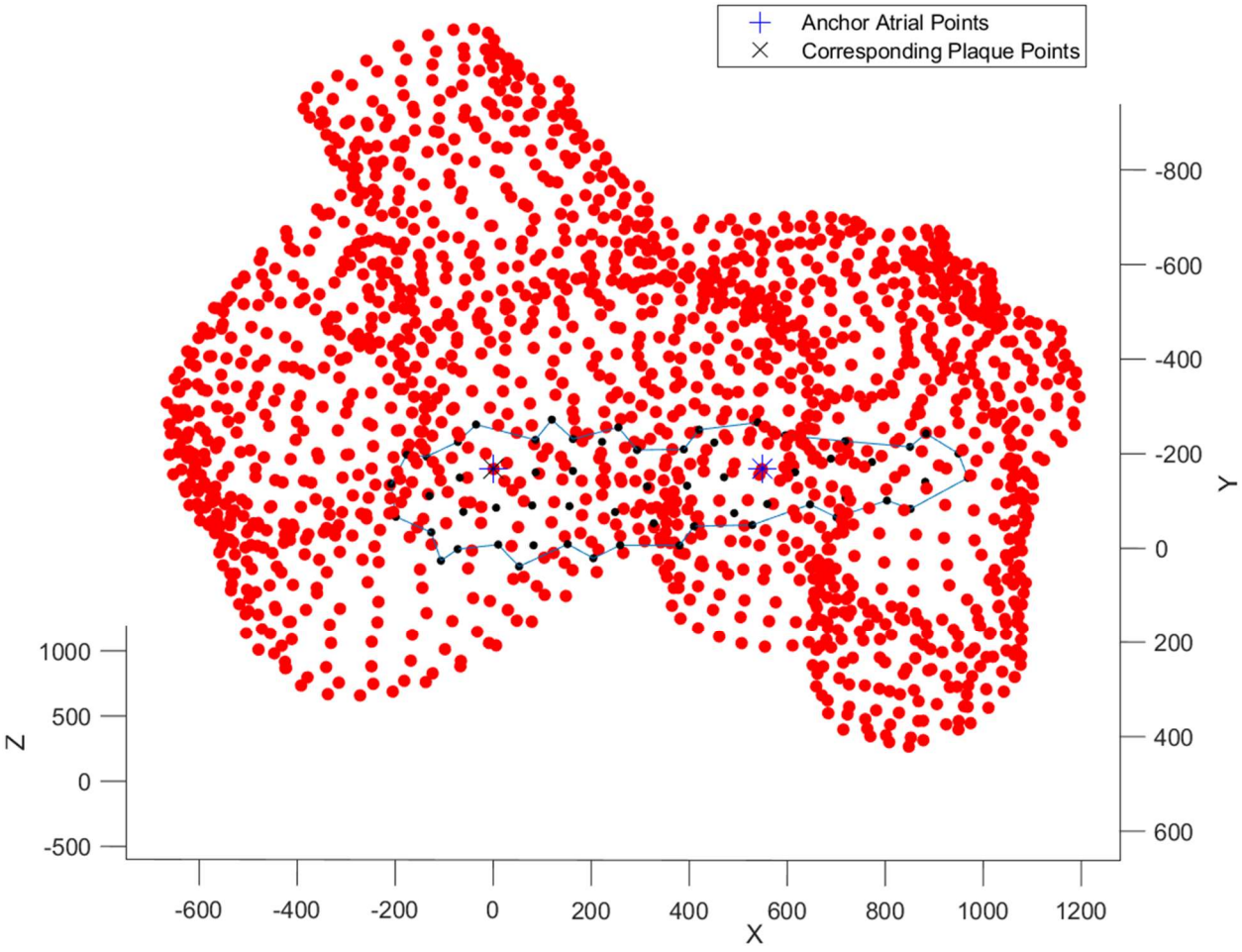

Figure 3.15: Plaque and Atria Geometry Plot after first mesh rotation

Figure 3.16 shows the geometry after the second mesh rotation. The biatrial plaque is now positioned parallel to its corresponding atrial mesh area. The two anchor points are still matched to the plaque points and there is no distortion in the shape of the mesh.

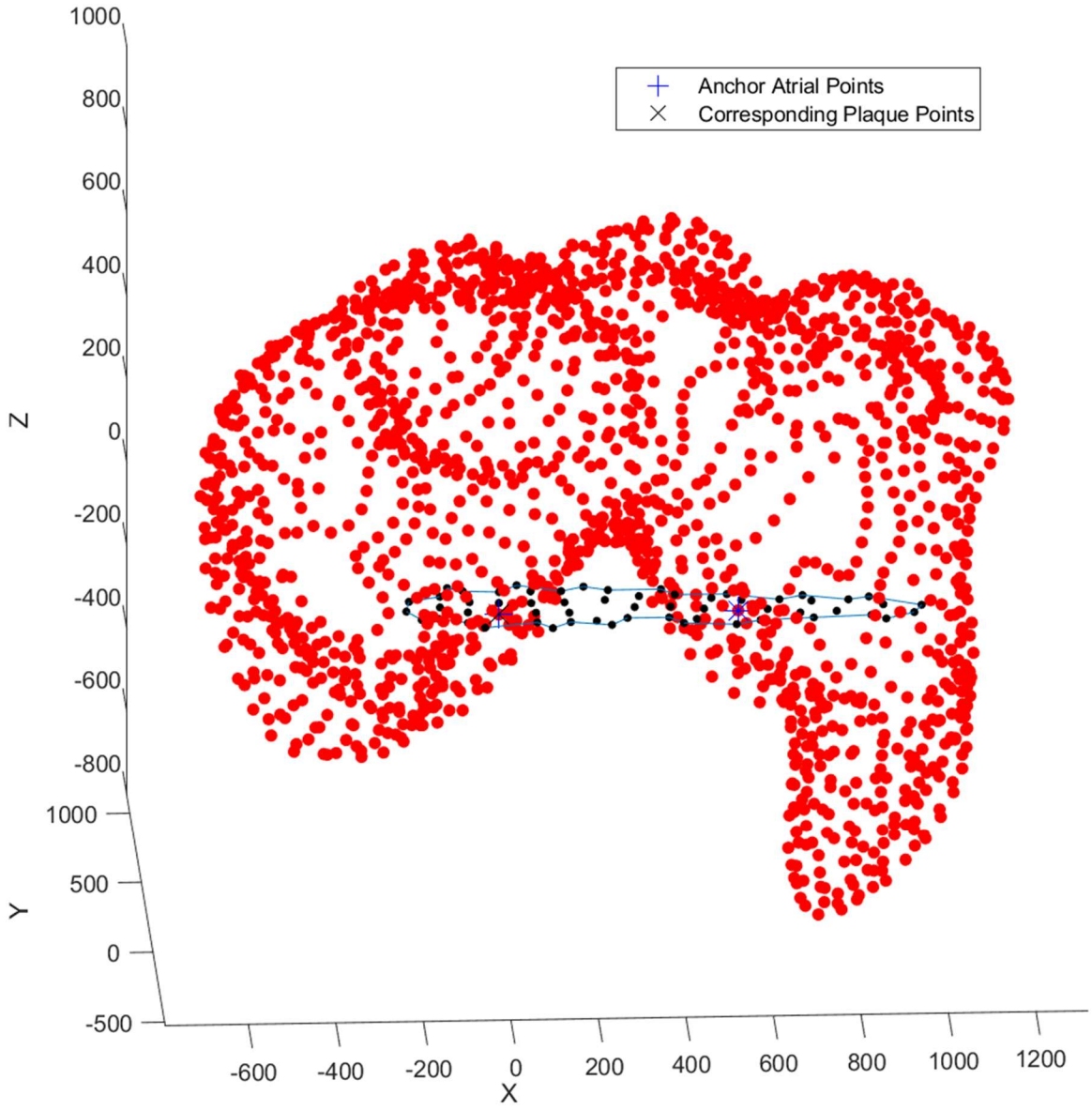

Figure 3.16: Plaque and Atria Geometry Plot after second mesh rotation

3.2.3 Projection and Interpolation of Atrial Vertices

Once the plaque and the atrial mesh are aligned as desired, the atrial mesh points are projected onto the 2D plaque plane (i.e., xy plane). The vertical distance threshold between the

mesh point and the plaque plane is adjusted such that the mesh point on the other side of the atria is excluded from the points to be projected (Figure 3.17).

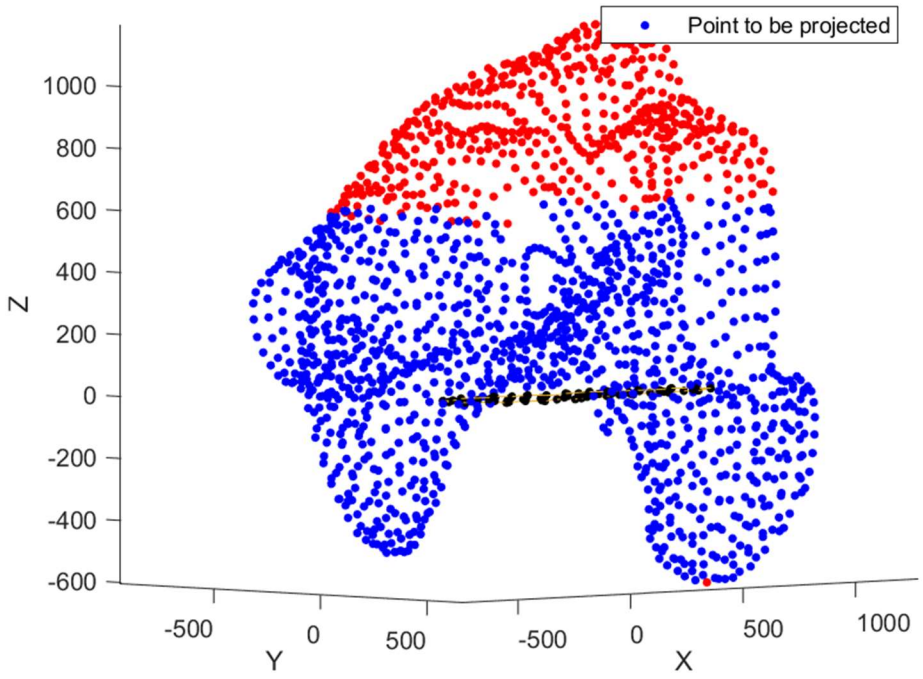

Figure 3.17: Threshold was adjusted so that the points on the opposite side of the atria (red) is not considered for the projection.

Once the threshold is determined, the atrial mesh points are vertically projected onto the 2D plaques, and the points that falls within the boundary of the plaque are chosen for interpolation (Figure 3.18). Figure 3.19 shows the positions of the chosen atria points relative to the reference electrode plaque position, suggesting the atria vertices at the correct area were chosen. There is a slight discrepancy between the electrode (in blue) area and the chosen atrial points (in green) area. This is due to the possible differences in geometry between the idealized electrode used for reference and the actual electrode position in the OR. However, the idealized electrode geometry can still be used to approximate the area where the plaque was placed.

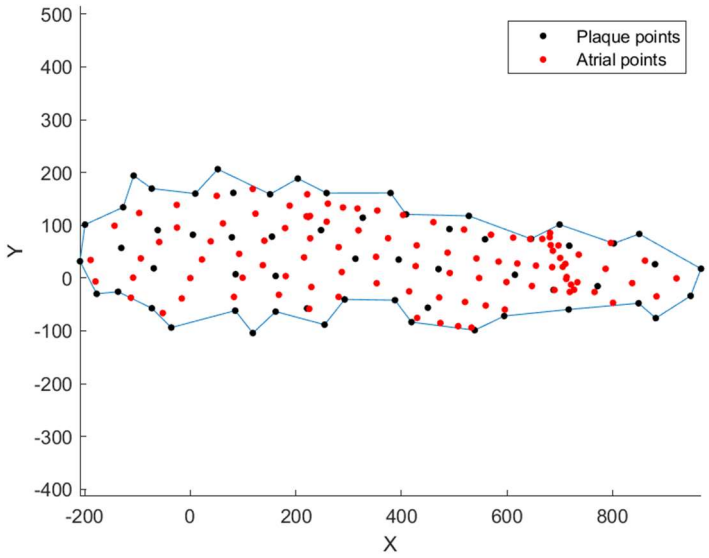

Figure 3.18: 2D plaque (black) and the chosen projected atrial points (red). Only points that are within the boundary (in blue) is considered for interpolation.

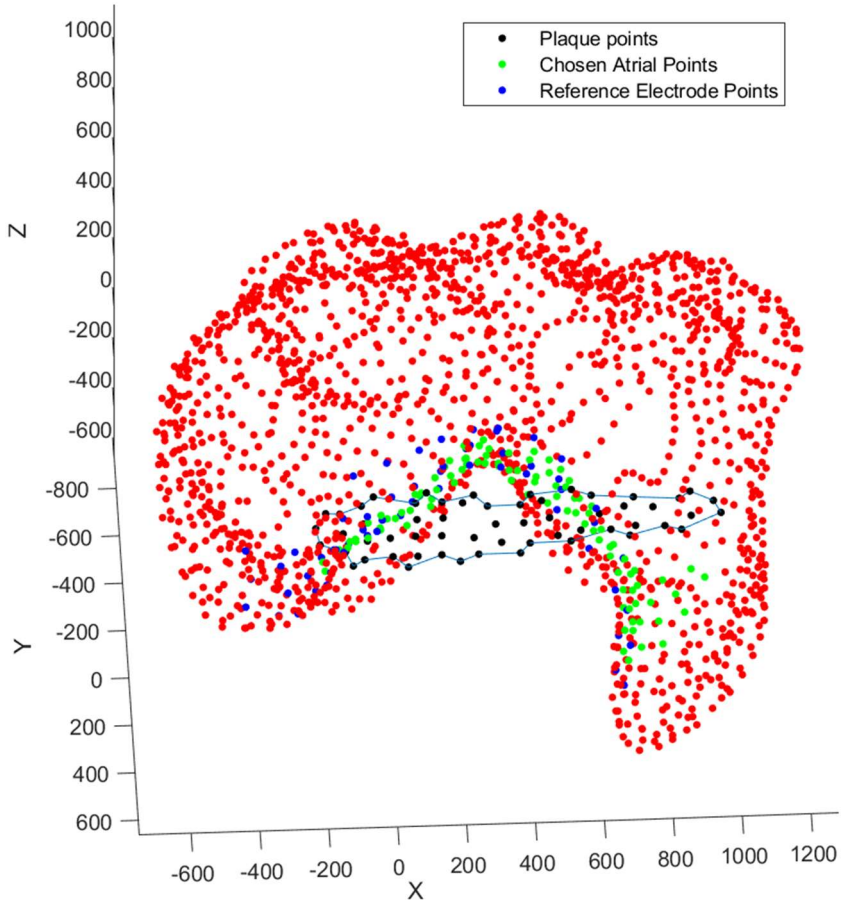

Figure 3.19: 3D geometry showing that the chosen atrial points (green) are within the area determined by the reference biatrial electrode plaque (blue)

Interpolation is done to derive the value (i.e., activation time) of the projected atrial points (Figure 3.20). The atria point activation time is consistent with that of the electrodes, suggesting the interpolation successfully derives the activation time (or values) of the atrial points.

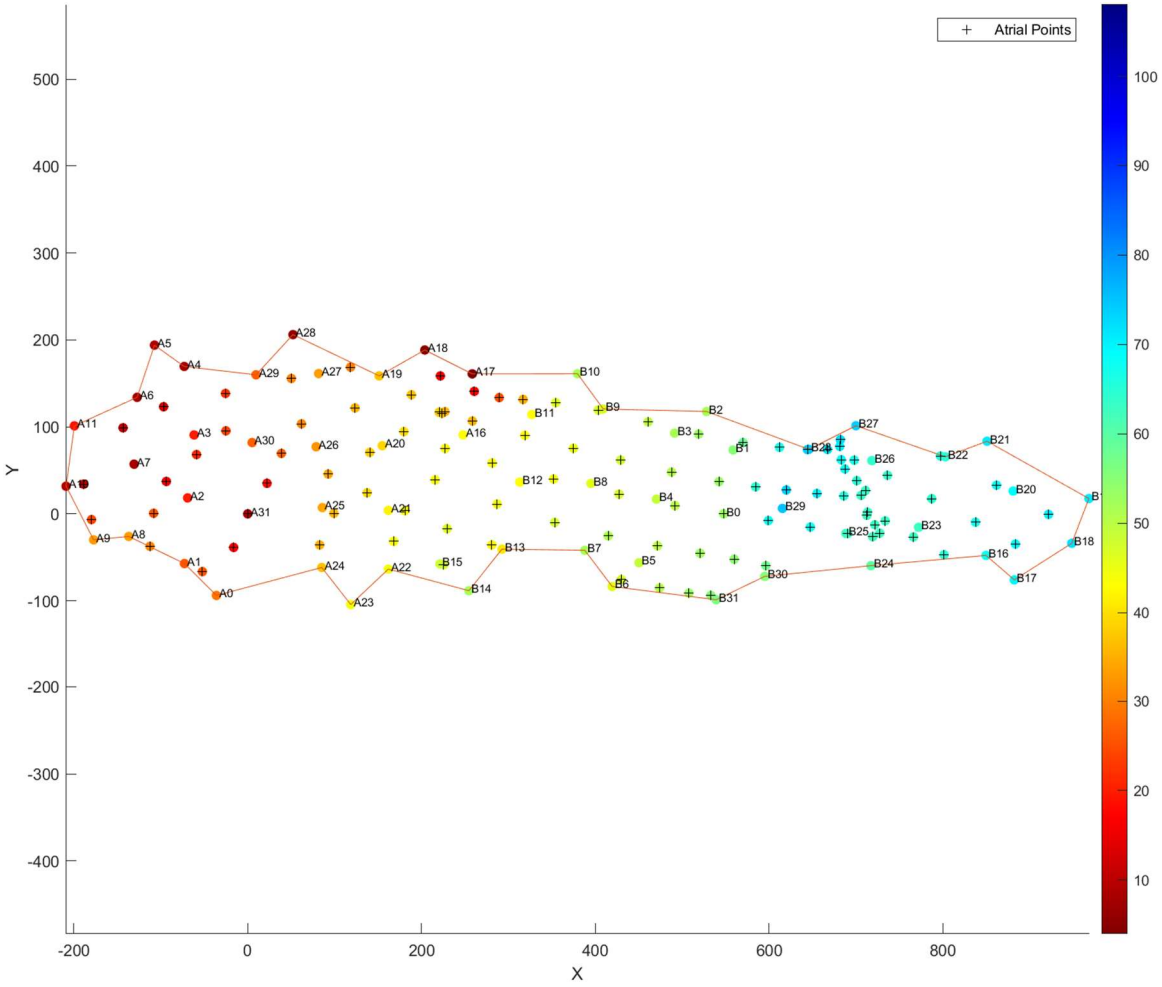

Figure 3.20: Distribution of the activation time in the biatrial plaque. The points with black cross are interpolated atrial points. Electrode points has its Intan number indicated next to it.

3.2.5 Visualization

The procedure of transformation, projection, and interpolation is repeated for three plaques to obtain the interpolated atrial activation time at all three plaques. The activation time map is plotted using these interpolated values. The triangulations that were used to render the 3D geometry of the atria are kept in the activation map instead of smoothing out the edges. This is to prevent errors in the interpretation of the color map (Figure 3.21). *interp* shading smooths out the edges of the triangulation in *trisurf* plot by interpolating the color value across different edges. This results in the boundary of the plaques getting interpolated values that is not representative of the actual value collected, creating red edges around all the plaques, disrupting accurate interpretation of the map. Therefore, shading the *trisurf* was kept as *flat* instead of *interp.*

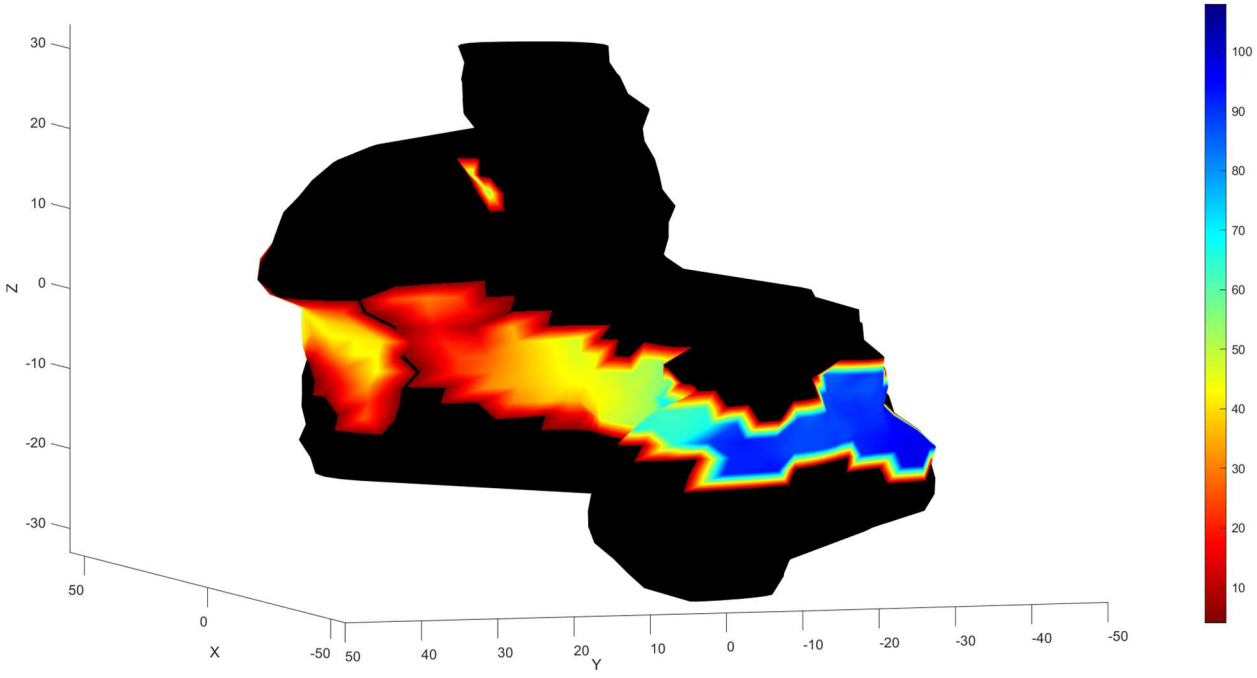

Figure 3.21: Smoothing out the triangular edges causes an interpolation of edge values, creating red edges around the plaques, affecting accuracy of the map.

The activation time map is plotted using these interpolated values, without smoothing out the triangulation edges (Figure 3.22 for RP plaque, 3.23 for LP plaque, and 3.24 for biatral plaque). There is a consistent trend in the activation time across the atria starting from the RAA where the stimulus was applied. Starting from RAA, the activation wavefront travels down the right atrium (Figure 3.22) and then across to the left atrium (Figure 3.23). Another wavefront also starts at RAA but travels across to the biatrial area (Figure 3.24). This activation wavefront travels across biatrial plaques toward the left side of the atria. With a constant color scale across all three plaques, the left side of the atrium has almost simultaneous activation (Figure 3.23a). Adjusting the limit of the color map scale reveals that the activation wavefront approaches from the top and left of the LP plaque (coming from the RAA and biatrial plaque) first before the rest of the area is activated (Figure 3.23b).

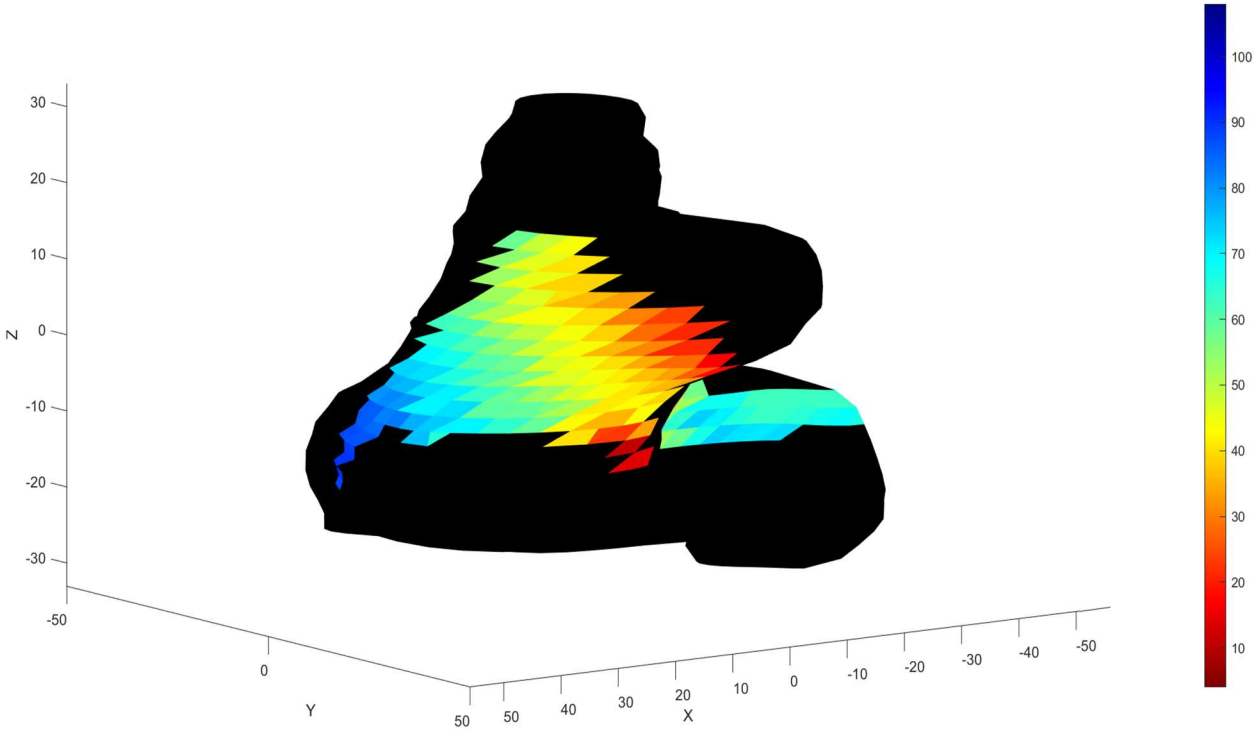

Figure 3.22 Activation map showing RP Plaque

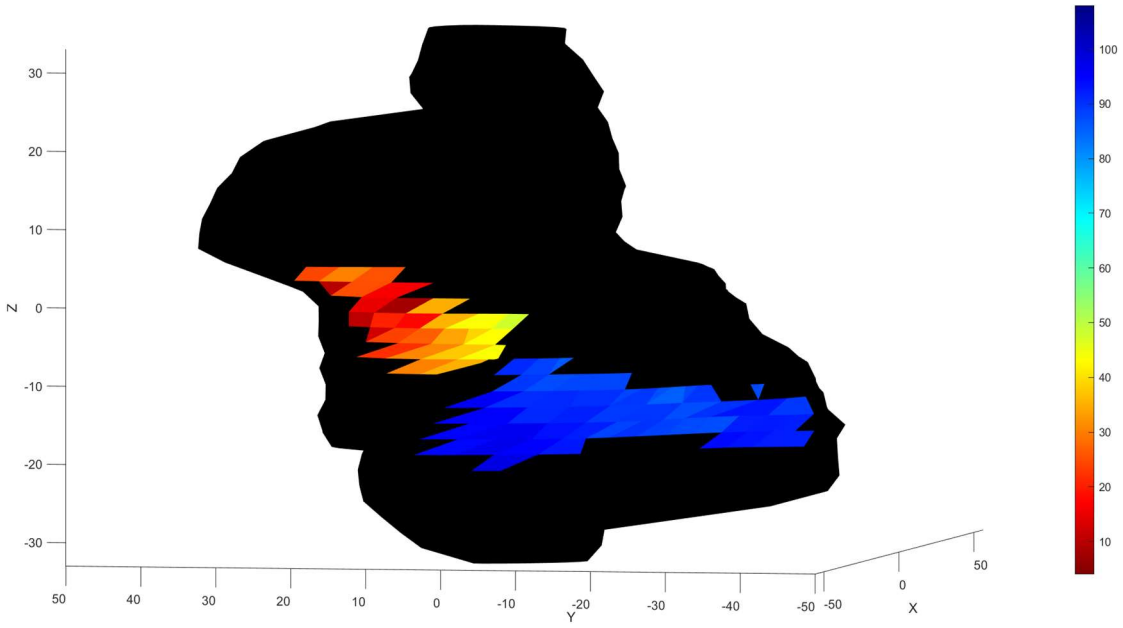

(a)

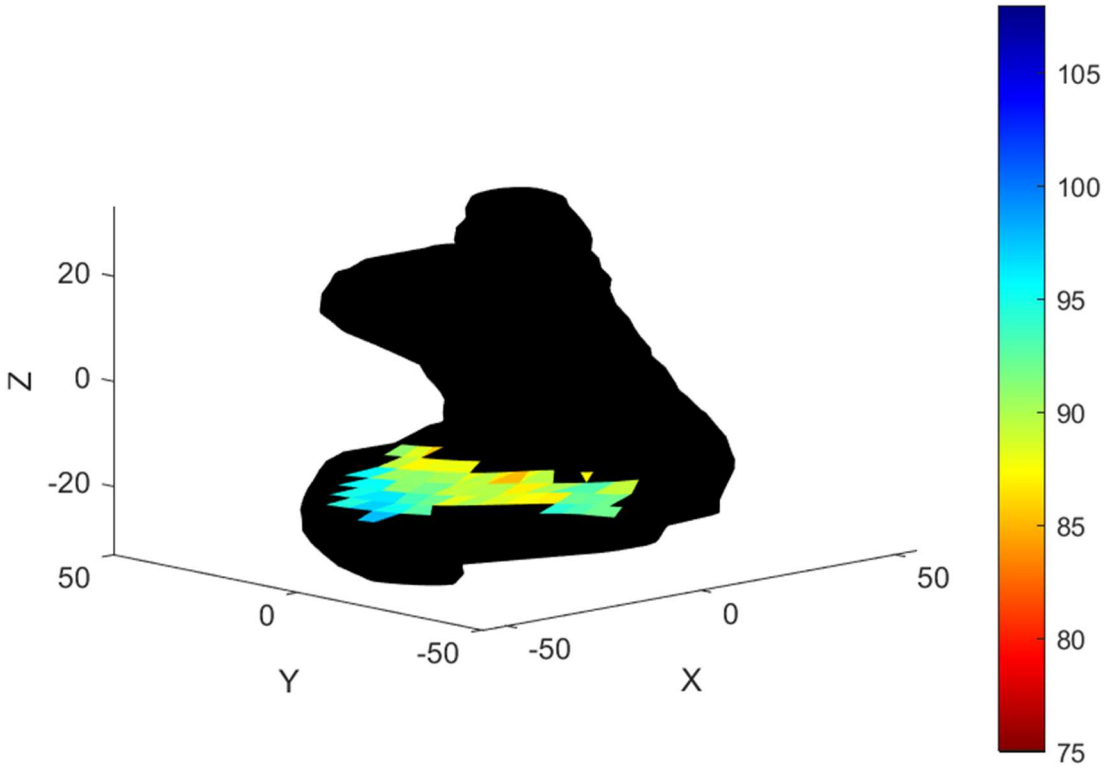

(b)

Figure 3.23 Activation map showing LP Plaque with (a) color map scale consistent with the other plaques (b) color map scale is adjusted to reveal more details of activation time.

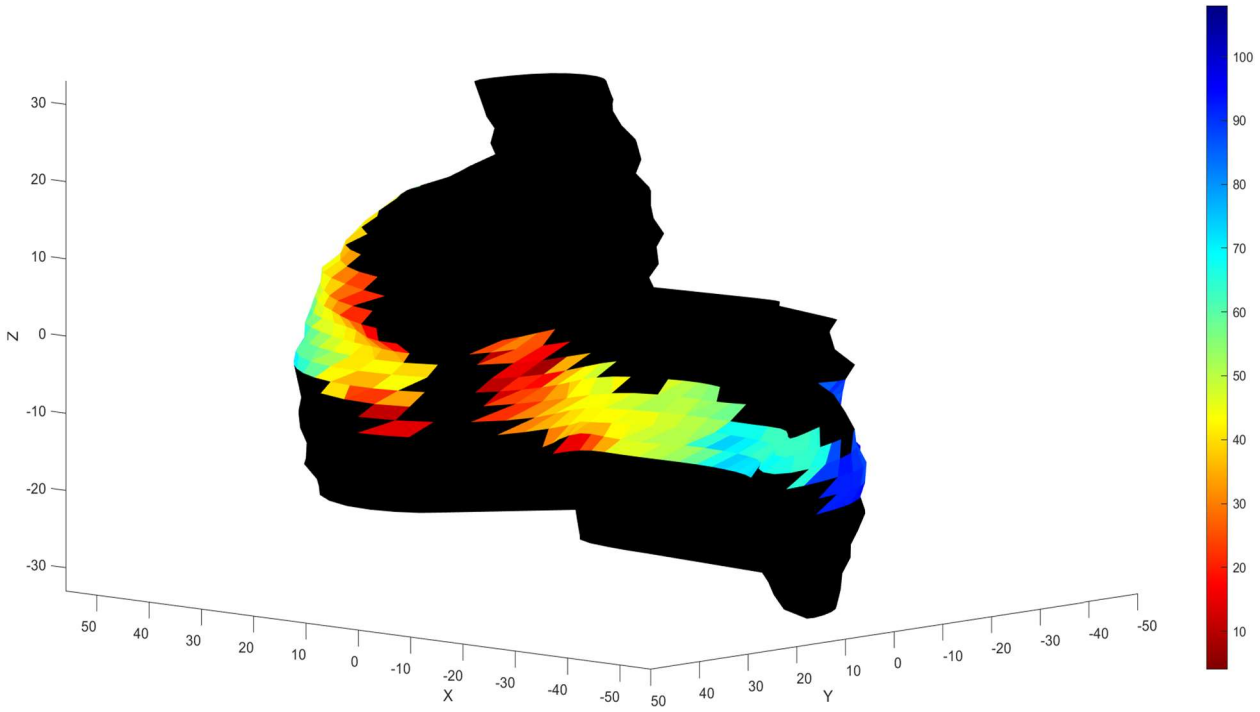

Figure 3.24 Activation map showing Biatrial Plaque

Chapter 4: MATLAB GUI Overview

The workflow described in Chapter 2: Method to load and process signal, calculate activation time, transform plaque and atria geometry, project and interpolate atria vertex points and generate activation map is incorporated into a MATLAB GUI for accessible use of the workflow in the lab. The view of the GUI is shown in Figure 4.1. There are a total of three tabs in the MATLAB GUI: Pre-processing, Transformation, Projection and Interpolation, and Visualization (Figure 4.1)

4.1 Pre-processing Tab:

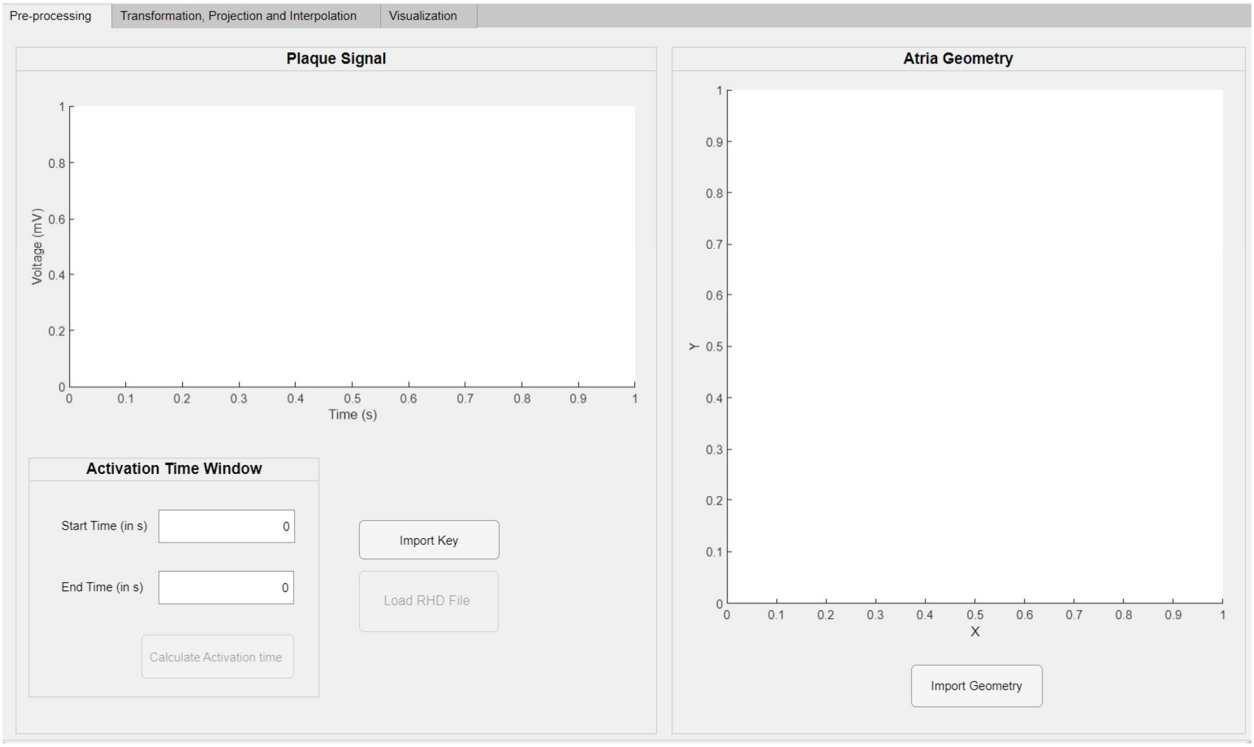

Figure 4.1: MATLAB GUI starting screen (Pre-processing Tab). There are three tabs indicating three steps of the workflow.

The MATLAB GUI starts with Pre-processing Tab (Figure 4.1) where relevant data including reference geometry, Intan key and the RHD signal file is loaded. The signal will get processed, and the activation time is calculated at this stage. Users start by clicking the "Import Geometry" button (Figure 4.1) which prompts users to load the reference atrial and electrode geometry (Figure 4.2). The "Import Key" allows loading of Intan Key files. The key needs to be loaded first before being able to load the RHD file from Intan output. 60 Hz filter will be applied on loading the RHD file before the filtered data gets plotted (Figure 4.2)

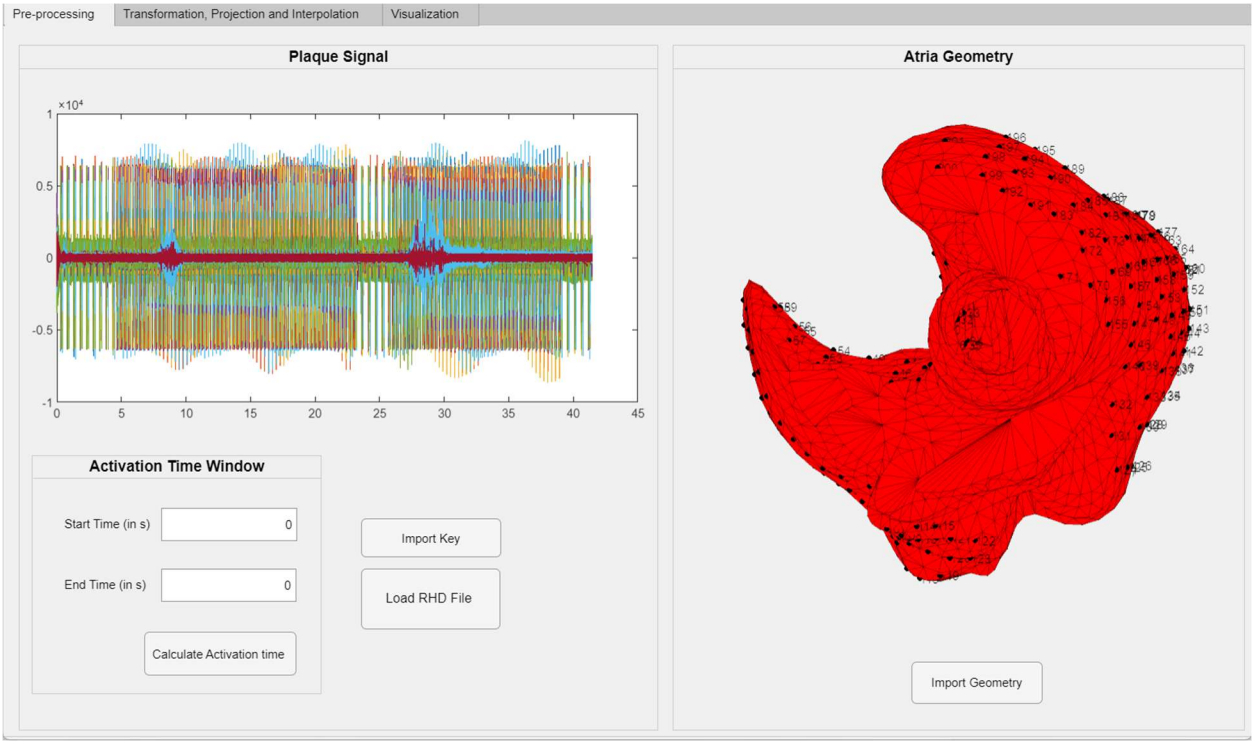

Figure 4.2: Reference geometry is displayed in the Atria Geometry panel after loading the geometry via "Import Geometry" button. Filtered signal is displayed in the Plaque Signal panel after the key and RHD file is loaded.

After manually determining the activation time window from the plot in the Plaque Signal panel, the activation start, and end time can be inputted in seconds (Figure 4.3). After the start and end time is entered, the "Calculate Activation Time" button starts the activation time

calculation using the method described above, and the signal within the activation time is displayed in the Plaque Signal panel (Figure 4.3).

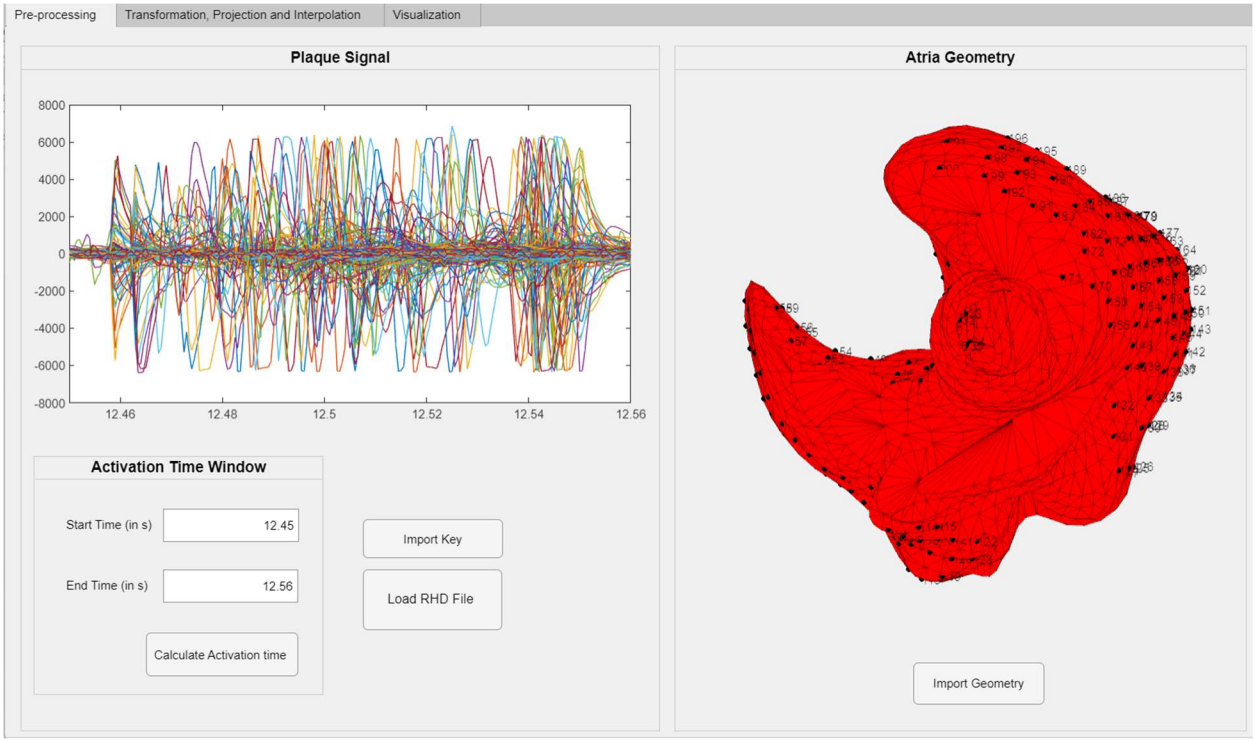

Figure 4.3: Start and End Time (in s) can be entered in the Activation Time Window panel. After Activation time is calculated, the signal plot will displayed the signal within the window of interest.

4.2 Transformation, Projection, and Interpolation Tab:

After the Activation Time is calculated, users can move to Transformation, Projection and Interpolation Tab (Figure 4.4). In this tab, users would be able to transform the plaque and atria geometry to align the plaque to its position on the atria mesh for projection and interpolation. Users start by choosing the plaque they want to map before clicking the “Map” button to plot the plaque onto the axis (Figure 4.5)

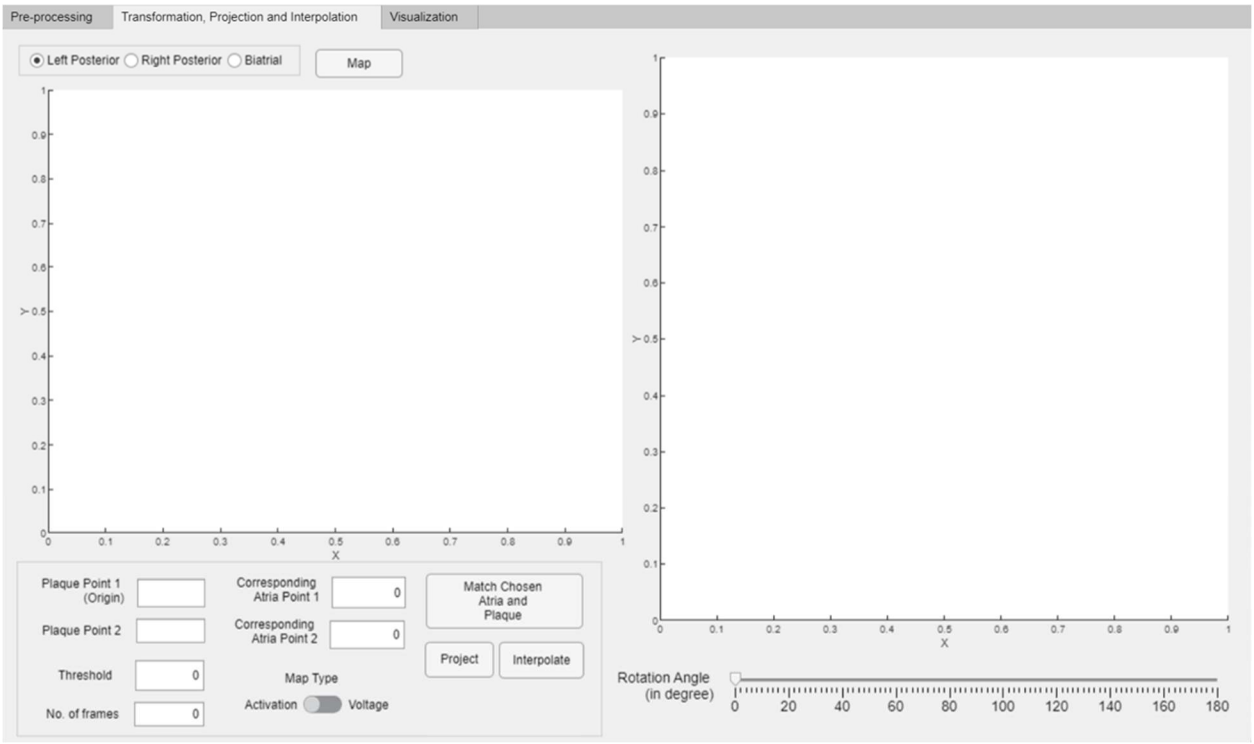

Figure 4.4: Transformation, Projection and Interpolation Tab

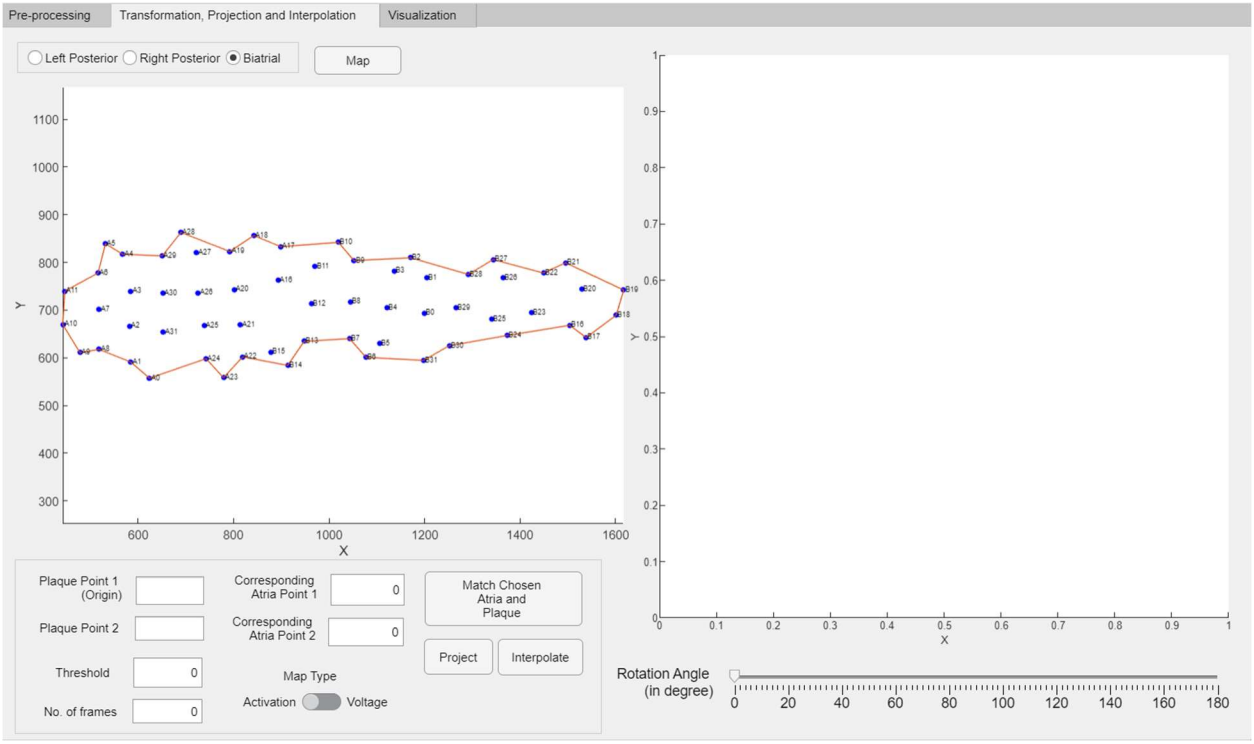

Figure 4.5: Plaque of interest is chosen. “Map” button shows the geometry of the plaque.

The anchor – plaque point pair corresponding to the chosen plaque (refer to Table 1) is entered in order to perform the transformation to match the anchor points and plaque via the "Match Chosen Atria and Plaque" Button. The atria and plaque geometry after the transformation is displayed in the axis on the right (Figure 4.6). Users can rotate the map to ensure that the anchor – electrode pairs of interest are matched as expected. Once that is confirmed, the "Rotation Angle" slider can be used to rotate the atria mesh around the x-axis (or A_pB_p vector). Users can rotate the atria until the desired position of the atria relative to the plaque is achieved.

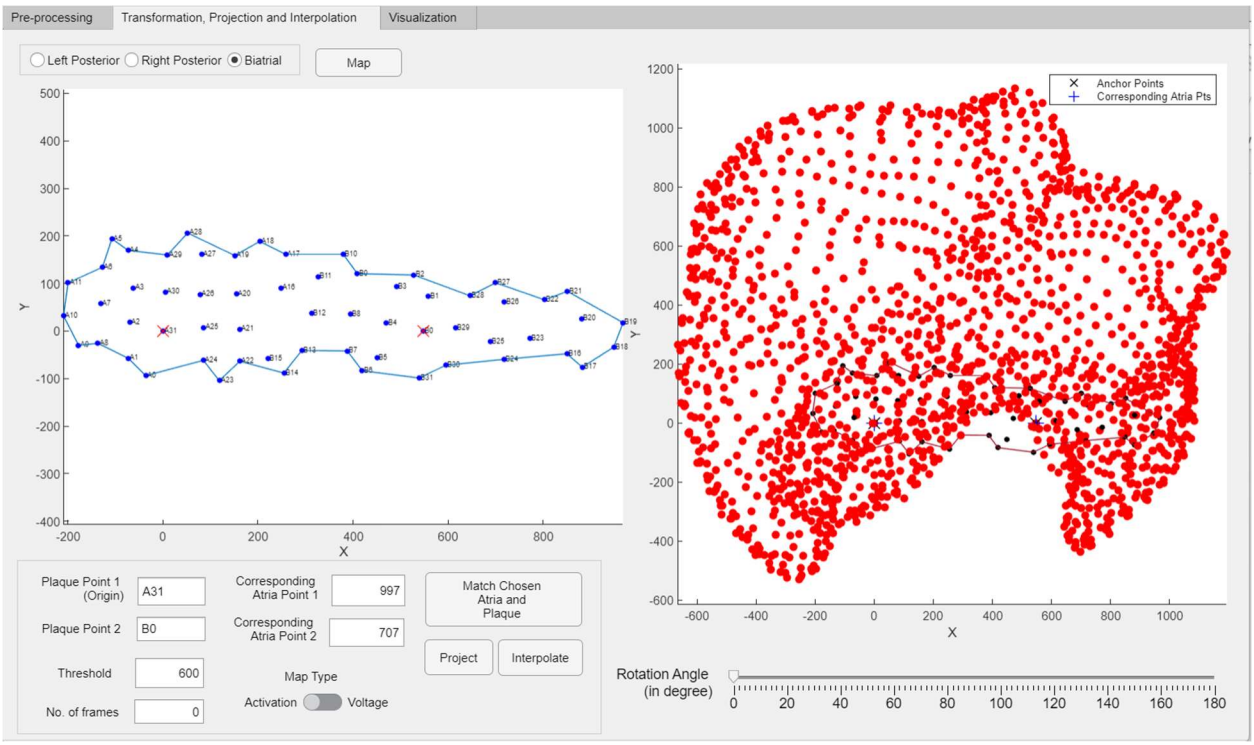

Figure 4.6: Once anchor – plaque points pairs are entered, the atria and plaque points are matched. The geometry after transformation is displayed in the axis on the right. Rotation Angle (in degree) slider is used to rotate the atria geometry around the x-axis to position the atria relative to the plaque in preparation for projection and interpolation.

Once plaque and atria geometry are aligned as desired, the projection threshold is entered before initiating the projection of atrial points onto the plaque plane. Chosen projected atrial

point on the plaque plane is displayed on the left axis while the position of the chosen atrial points in 3D is displayed on the right axis for users to verify its position relative to the reference electrode plaque (Figure 4.7). A figure similar to Figure 3.13 will also be displayed to allow users to verify if the chosen threshold is optimal.

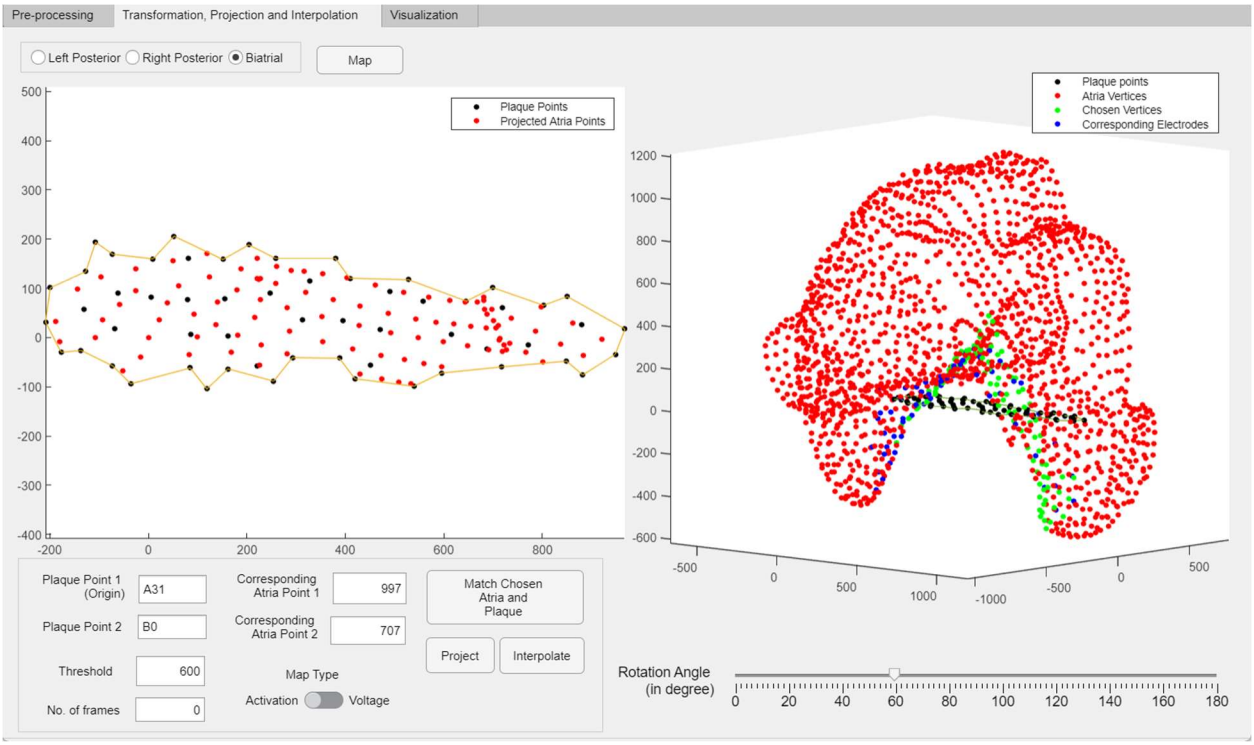

Figure 4.7: Axis on the left displayed the projection of the chosen atrial point on the plaque plane. Axis on the right display the 3D position of the chosen atrial point in relation of reference electrode points for verification.

Once the chosen atrial points are verified, users can initial interpolation which will display the interpolated values of the atrial points in relation to the values of the plaque points in 2D (Figure 4.8). Pressing the “Interpolate” button would also save the interpolated value for use in visualization in the Visualization tab. Therefore, users need to make sure that they choose the right type of Map before they initial interpolation process. Figure 4.8 shows that the activation map is chosen. Only the “Activation” map option displays the interpolated value for verification. For the “Voltage” map, the number of frames need to be indicated before interpolation.

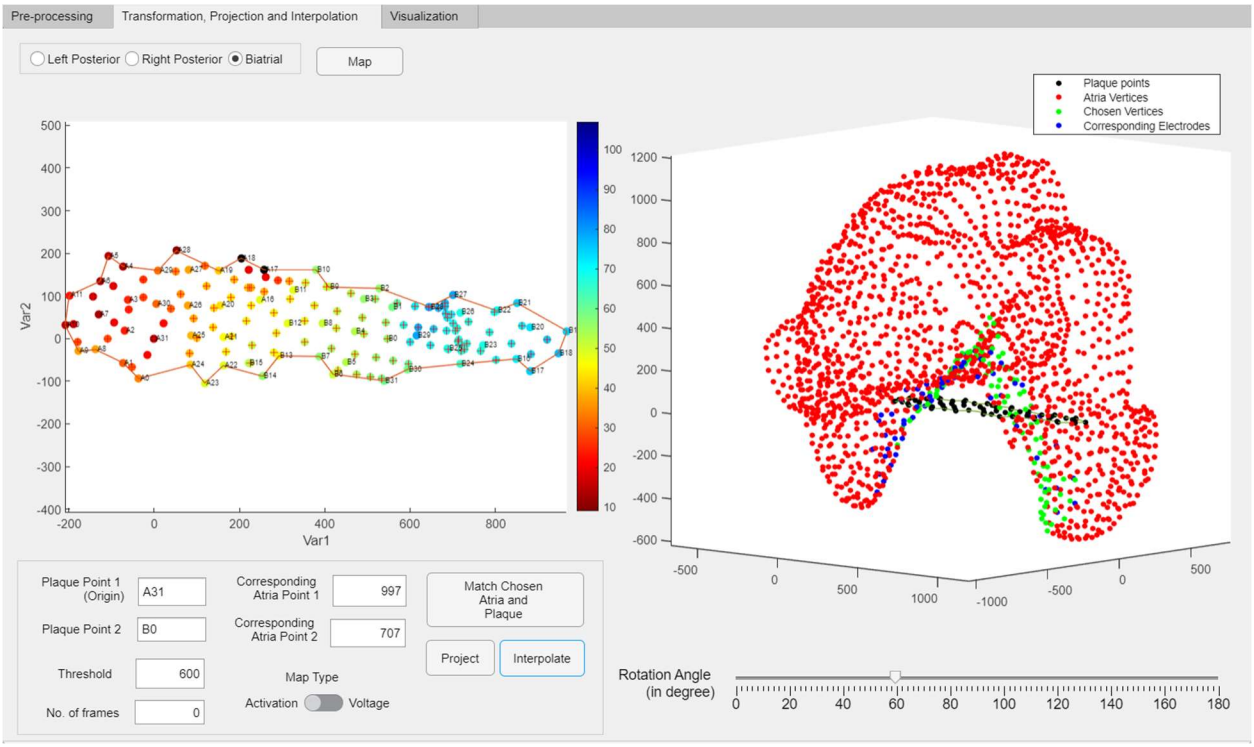

Figure 4.8: Interpolated activation time displayed in relation to that of the plaque points with "Activation" map as the chosen map type .

4.3 Visualization Tab:

Any plaque undergoing the process in the Transformation, Projection, and Interpolation tab described in 4.2 will be loaded into Visualization Tab for 3D visualization using the reference geometry loaded in Pre-processing Tab. There are options to generate activation map and voltage map videos. Activation map will be displayed on the axis if the "Generate Activation Map" button is chosen (Figure 4.9). For the "Generate Voltage Map Video" option, users can choose a preset view for the generated view. This option will generate a video ('voltagemap.avi') displaying the changes in voltage across the chosen window using the total number of frames indicated in the previous tab. Voltage Map generated will have a framerate of 5 fps.

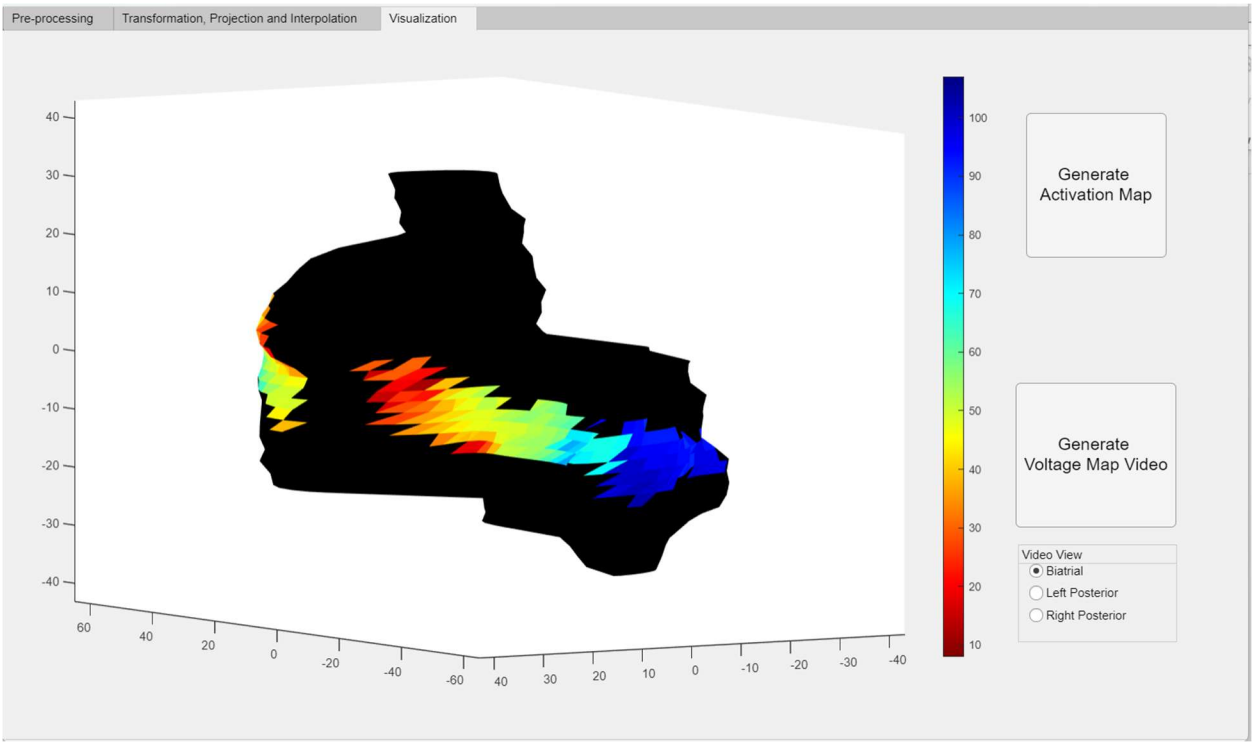

Figure 4.9: Visualization Tab with Activation Map generated and displayed on the axis.

Chapter 5: Discussion

The study design has been successful in rendering a visualization of the 2D electrode plaque signal on the 3D atrial geometry. The 3D visualization shows an expected pathway for electrical conduction in the atria in response to the pacing signal. The signal travels from the pacing point in RAA down the right atria and over to the biatrial area before reaching the left atrium. Moreover, the processing and visualization of the input data have allowed us to understand the nature of the input signal from the Intan Recording System. Noisy channels have been investigated and troubleshooted to produce more meaningful datasets. For future study, there are still rooms for improvement in signal processing and transformation. This includes filtering for noisy channels and channels with poor atrial contact, evaluating different methods to obtain the activation time, and isometrically transforming the 2D plaque to match the curvature of the 3D atrial geometry.

Firstly, the signal processing design was able to remove most of the noise, especially power line noise, from the input signal through a 60Hz notch filter. The filtered signal shows clear peaks which allow for the detection of the activation time as the maximum voltage. However, from the superimposed plot of the filtered signal from all the channels in Figure 3.1b, there is still presence of low amplitude noise. This does not affect the determination of the activation time done in this study since clear absolute peaks are not covered by low amplitude noise. However, with other methods of identifying activation time with higher accuracy such as maximum negative slope, this baseline noise can be disruptive. In the future, filters can be developed to remove more baseline noise from the filtered signal. Since the noise is of much

different frequency from the actual signal of interest, noise frequency can be identified, and filters can be designed to remove them. Moreover, Adaptive Noise Cancellation (ANC) filters, which include a filter and an adaptive algorithm, have been studied as an advanced method for noise filtering, especially power line noise, baseline wanders or motion artifacts [12] This can be another possible method for more advanced noise filtering moving forward.

Secondly, while most of the channels from the Intan Recording System have signals with clear peaks, there are still a small number of channels that are pure noise and do not contain meaningful signals. There is no method in this study to recognize these noisy signals and remove them. In future studies, a plan can be devised to recognize the noisy channels and remove them from the datasets. Z-score is a possible metric that can be used to filter out noisy channels. Z-score measures the deviation from the mean of the population; therefore, a threshold can be set to remove the channels that deviate from the rest of the channels. Z-score has already been proven effective in removing bad channels in ECGI software [10]

As mentioned previously, absolute maximum voltage was used as the method of calculation because of its robustness as well as because our signals have very clear peaks that enable higher accuracy. However, for future studies, different methods for activation time calculation can be applied to the design plan. Evaluation of different calculation methods can be useful in devising the optimal activation time calculation method.

Scatterplots for activation time distribution in the plaques reveal problems of poor contact between the plaque electrodes and the atria. Poor contact prevents the electrodes from detecting the atrial activation signal, resulting in inaccurate activation time calculation. Early detection of

these points in the signal processing procedure prevents the need for manually removing these channels from the list of channels at a later time. A possible design can be to set a threshold for the absolute maximum voltage to remove electrodes that do not detect an actual atrial activation.

The design of the transformation matrix shows accuracy in matching the anchor points and the plaque electrodes. Although this study defines the anchor – plaque point pairs based on the rendered 3D geometry, there is high confidence that the algorithm is able to match any pairs of 2D plaque points and 3D atrial anchor points, ensuring its ability to match the geometry with anchor – plaque point pairs given by the surgeons. One way in which our current matching of the plaque and atrial geometry can be improved is to allow for isometric bending of the plaques, e.g., into a parabolic shape. Anchor – plaque pairs should not be chosen at the ends with our current approach because high atrial geometry can lead to a significant mismatch. This problem is especially pronounced for the biatrial plaque which attaches to a particularly curved part of the atria. Future improvements can be made to the plaque transformation to take into account the curvature of the atria.

Chapter 6: Conclusion

Overall, the algorithm and the MATLAB GUI have been successful in achieving the two aims laid out previously: loading, processing, and visualizing the input signal from the Intan recording system for understanding of the nature of the signal and troubleshooting the data acquisition system and projecting the 2D signal values onto 3D geometry to understand the dynamic of the electrical conduction in the atria. Filtered signals provide a meaningful understanding of the electrical activity of the heart, specifically in the calculation of the activation time at each plaque electrodes. The 3D visualization of the interpolated values achieved the expected integration of the data from all three plaques that greatly facilitates interpretation. For future works, there is room for improvement in signal processing to further remove noise and improve the signals as well as in transformation design to consider the curvature of the atria geometry. It is also straightforward to extend the application of this approach to generate other useful maps for arrythmia study, including phase mapping of the atria and action potential duration.

References

1. Desai DS, Hajouli S. Arrhythmias. In: StatPearls [Internet]. Treasure Island (FL): StatPearls Publishing; 2023. Available from: http://www.ncbi.nlm.nih.gov/books/NBK558923/

2. Fu DG. Cardiac Arrhythmias: Diagnosis, Symptoms, and Treatments. Cell Biochem Biophys. 2015 Nov; 73(2):291-296. doi: 10.1007/s12013-015-0626-4. PMID: 25737133.

3. Lippi G, Sanchis-Gomar F, Cervellin G. Global epidemiology of atrial fibrillation: An increasing epidemic and public health challenge. International Journal of Stroke. 2021;16(2):217–21.

4. Sagris M, Vardas EP, Theofilis P, Antonopoulos AS, Oikonomou E, Tousoulis D. Atrial Fibrillation: Pathogenesis, Predisposing Factors, and Genetics. IJMS. 2021 Dec 21;23(1):6.

5. Blumenthal R, Calkins H. Atrial Fibrillation: Prevention, Treatment and Research [Internet]. Johns Hopkins Medicine. 2022. Available from: https://www.hopkinsmedicine.org/health/conditions-and-diseases/atrial-fibrillation-prevention-treatment-and-research

6. American Heart Association. What is Atrial Fibrillation? [Internet]. www.heart.org. Available from: https://www.heart.org/en/health-topics/atrial-fibrillation/what-is-atrial-fibrillation-afib-or-af

7. Kligfield P. The centennial of the einthoven electrocardiogram. Journal of Electrocardiology. 2002 Oct;35(4):123–9.

8. Reichlin T, Abächerli R, Twerenbold R, Kühne M, Schaer B, Müller C, et al. Advanced ECG in 2016: is there more than just a tracing? Swiss Medical Weekly. 2016 Apr 24;146(1718):w14303–w14303.

9. Rudy Y. Noninvasive ECG imaging (ECGI): Mapping the arrhythmic substrate of the human heart. Int J Cardiol. 2017 Jun 15;237:13-14. doi: 10.1016/j.ijcard.2017.02.104. Epub 2017 Feb 27. PMID: 28258845; PMCID: PMC5441950.

10. Ramanathan C, Ghanem RN, Jia P, Ryu K, Rudy Y. Noninvasive electrocardiographic imaging for cardiac electrophysiology and arrhythmia. Nat Med. 2004 Apr;10(4):422–8.

11. Milani-Nejad N, Janssen PML. Small and large animal models in cardiac contraction research: Advantages and disadvantages. Pharmacology & Therapeutics. 2014 Mar;141(3):235–49.

12. Martinek R, Ladrova M, Sidikova M, Jaros R, Behbehani K, Kahankova R, et al. Advanced Bioelectrical Signal Processing Methods: Past, Present and Future Approach—Part I: Cardiac Signals. Sensors. 2021 Jul 30;21(15):5186.